Professor Efstratios Pistikopoulos
Centre for Process Systems Engineering
Imperial College London

Professor Wolfgang Marquardt
Institute for Process Systems Engineering
RWTH Aachen University

Professor Constantinos Pantelides
Process Systems Enterprise
Managing Director

Capital Cost Evaluation for Optimum Process Design of Cryogenic Air Separation

Diploma Thesis
by
Robert Pack

London, SS 2012

Diploma Thesis
for
Mr. Robert Pack

Task Description

Current air separation process optimization is carried out sequentially with various discrete or continuous process parameters, and then iterated with equipment sizing and costing. Typical process parameters include temperature, pressure, flow, pressure drop, product purity, distillation column feed and/or draw locations staging, and etc. Major equipment used in cryogenic air separation include air compressors, turbines, plate and fin heat exchangers, cooler, distillation columns, condensers, reboilers, and etc. Once process optimum condition is identified, individual equipment is sized and cost estimated. Capital cost is then feed back to process to verify the original optimum condition. If the original optimum condition changes, we will have to re-optimize the process parameter and identify the new process optimum condition. New equipment sizing and costing will have to be adjusted accordingly.

The deficiency of the current process is apparent: manual, sequential and iterative. We would like to streamline the optimization process, incorporate the capital equipment cost into the process optimization. The process optimizer we target is gPROMS. The goal is to simultaneously optimize process and equipment to minimize the total process cost with user defined objective functions.

Prof. Efstratios Pistikopoulos

Prof. Dr.-Ing. Wolfgang Marquardt

Betreuer der Arbeit: Dipl. Ing. Mirko Skiborowski
Tag der Abgabe: xx.xx.2012

Statutory Declaration

I herewith declare that I have completed the present thesis independently making use only of the specified literature and aids. Sentences or parts of sentences quoted literally are marked as quotations; identification of other references with regard to the statement and scope of the work is quoted. The thesis in this form or in any other form has not been submitted to an examination body and has not been published.

Date Signature

Contents

List of Figures

List of Tables

Nomenclature

POT	Payout time	[$]
a	Annuity	[$]
C_0	Initial value of an investment	[$]
C_n	Final value of an investment	[$]
C_{0e}	Present value of all expenses	[$]
C_{0r}	Present value of all revenues	[$]
i	Interest rate	[%]
NPV	Net present value	[$]
q	Interest factor	[−]
$\dot{e}_{ij}$	Energy flow of to equipment i from energy carrier j	$[kW]$
$\dot{m}_i$	Mass flow of component i	$[\frac{kg}{s}]$
C_B^i	Reference cost of equipment i	[$]
C_E^i	Cost of equipment i	[$]
C_{EC}^i	Mass specific cost of energy carrier i	$[\frac{\$}{kW}]$
C_{RM}^i	Mass specific cost of raw material i	$[\frac{\$}{kg}]$
C_1	Reference equipment cost at time 1	[$]
C_2	Reference equipment cost at time 2	[$]
C_P	Total process cost	[$]
C_P^0	Reference process cost	[$]
C_{EC}	Total cost of energy	[$]

C_{FILL}	Cost of raw materials to fill the process	[$]
C_{RM}	Total cost of raw materials	[$]
f_C^i	Design complexity correction to equipment cost	[−]
f_M^i	Material selection correction to equipment cost	[−]
f_P^i	Pressure correction to equipment cost	[−]
f_T^i	Temperature correction to equipment cost	[−]
I_1	Cost index at time 1	[−]
I_2	Cost index at time 2	[−]
M^i	Equipment specific factor	[−]
N_E	Number of equipment pieces in the process	[−]
N_{RM}	Number of raw materials	[−]
Q^i	Specific quantity for equipment i	$[variable]$
Q_B^i	Equipment specific reference quantity	$[variable]$
Q_P	Process capacity	$[\frac{kg}{h}]$
Q_P^0	Reference process capacity	$[\frac{kg}{h}]$
t_{op}	Time of process operations	$[s]$
x	Degression coefficient	[−]

Constants

g	gravitational constant	$[\frac{m}{s^2}]$

Greek Letters

β	aeration factor	[−]
δ	film thickness	$[m]$
ϵ	packing void fraction	[−]
γ_i	liquid activity coefficient of component i	[−]

μ_G	vapour viscosity	$[Pa \cdot s]$
μ_L	liquid viscosity	$[Pa \cdot s]$
μ_S	isentropic expansion coefficient	$[\frac{K}{Pa}]$
μ_{JT}	*Joule-Thompson* coeffivcient	$[\frac{K}{Pa}]$
ν^D	reflux ratio	$[-]$
ν^R	boliup ratio	$[-]$
ν^{vap}	condenser vapour fraction	$[-]$
Φ	relative froth density	$[-]$
Ψ_{flood}	fractional allowed flooding	$[-]$
Θ	corrugation angle	$[rad]$
φ_i^0	reference vapour fugacity coefficient of component i	$[-]$
φ_i	vapour fugacity coefficient of component i	$[-]$
ζ_{ij}^L	splitting variable for liquid feed i on stage j	$[-]$
ζ_j^R	splitting variable for reboiler reflux on stage j	$[-]$
ζ_{ij}^{SL}	splitting variable for liquid side draw i on stage j	$[-]$
ζ_{ij}^{SV}	splitting variable for vapour side draw i on stage j	$[-]$
ζ_{ij}^V	splitting variable for vapour feed i on stage j	$[-]$

Variables

Δp	pressure drop over entire column	$[Pa]$
δp_{dry}	dry pressure drop	$[\frac{Pa}{m}]$
Δp_{stage}	stage-wise pressure drop	$[Pa]$
ℓ_{weir}	length of tray weir	$[m]$
a_c	parameter in Peng-Robinson EOS	$[\frac{m^5}{mol^2 s^2}]$
A_j^{min}	minimum column area on stage j	$[m^2]$

A_{active}	active tray area	$[m^2]$
b	parameter in Peng-Robinson EOS	$[\frac{m^3}{mol}]$
C_1	packing constant	[]
C_2	packing constant	[]
C_{column}	column cost	[$]
$C_{internals}$	cost of column internals	[$]
$C_{platform}$	platform cost	[$]
C_{tower}	tower cost	[$]
E	fractional weld efficiency	$[-]$
ent_j	fractional entrainment for 80% flooding on stage j	$[-]$
F_j^L	molar liquid feed flowrate to stage j	$[\frac{mol}{s}]$
F_j^V	molar vapour feed flowrate to stage j	$[\frac{mol}{s}]$
f_i^L	liquid fugacity	$[-]$
f_i^V	vapour fugacity	$[-]$
F_j^L	Liquid feed to tray j	$[\frac{mol}{s}]$
F_j^V	Vapour feed to tray j	$[\frac{mol}{s}]$
F_{Pi}	compressibility factor of component i	$[-]$
FLV_j	Sherwood flow parameter on stage j	$[-]$
h_j^L	molar liquid enthalpy on stage j	$[\frac{J}{mol}]$
h_j^V	molar vapour enthalpy on stage j	$[\frac{J}{mol}]$
h_j^{FL}	molar liquid feed enthalpy to stage j	$[\frac{J}{mol}]$
h_j^{FV}	molar vapour feed enthalpy to stage j	$[\frac{J}{mol}]$
h_f	froth height	$[m]$
h_L	dimesionless holdup	$[-]$

h_w	weir height	$[m]$
h_{ow}	height over weir	$[m]$
h_{plate}	plate spacing	$[m]$
$K1$	empirical coefficient	$[-]$
K_{ij}	equilibrium constant of component i on stage j	$[-]$
L_j	Liquid flow from tray j	$[\frac{mol}{s}]$
L_j	molar liquid flowrate form stage j	$[\frac{mol}{s}]$
l_{ij}	liquid molar flowrate of component i from stage j	$[\frac{mol}{s}]$
m	parameter in Peng-Robinson EOS	$[-]$
n_C	number of components	$[-]$
n_F	number of feeds	$[-]$
n_j^L	liquid molar holdup on stage j	$[mol]$
n_j^V	vapour molar holdup on stage j	$[mol]$
n_S	number of column stages	$[-]$
n_{ij}	holdup of component i on stage j	$[mol]$
p	pressure	$[Pa]$
p	system pressure	$[Pa]$
p_i^S	vapour pressure of component i	$[Pa]$
p_D	design pressure	$[psig]$
p_O	operating pressure	$[psig]$
S	corrugation side	$[m]$
S	maximum allowable stress	$[psi]$
S_j^L	molar liquid side-draw flowrate form stage j	$[\frac{mol}{s}]$
S_j^V	molar vapour side-draw flowrate form stage j	$[\frac{mol}{s}]$

s_j^V	dimensionless liquid side-draw from stage j	$[-]$
s_j^V	dimensionless vapour side-draw from stage j	$[-]$
S_j^L	Liquid side flow from tray j	$[\frac{mol}{s}]$
S_j^V	Vapour side flow from tray j	$[\frac{mol}{s}]$
T^{bub}	bubble point temperature	$[K]$
T^{dew}	dew point temperature	$[K]$
T^{sub}	sub-cooling temperature	$[K]$
t_p	shell thickness die to pressure	$[in]$
t_s	tower shell thickness	$[in]$
t_w	thickness wind and earthquake correction	$[in]$
U_j	internal energy holdup on stage j	$[J]$
v_G	vapour velocity	$[\frac{m}{s}]$
V_j	Vapour flow from tray j	$[\frac{mol}{s}]$
V_j	molar vapour flowrate form stage j	$[\frac{mol}{s}]$
v_j^{flood}	flooding velocity on stage j	$[\frac{m}{s}]$
v_L	liquid velocity	$[\frac{m}{s}]$
v_{ij}	vapour molar flowrate of component i from stage j	$[\frac{mol}{s}]$
V_{stage}	stage volume	$[m^3]$
W_{tower}	weight of a tower	$[lbs]$
x_{ij}	liquid mole fraction of component i on stage j	$[-]$
y_{ij}	vapour mole fraction of component i on stage j	$[-]$
y_i^{eq}	equilibrium vapour concentration of component i on stage j	$[\frac{mol}{mol}]$
z_{ij}^L	liquid mole fraction of liquid feed to stage j	$[-]$
z_{ij}^V	vapour mole fraction of vapour feed to stage j	$[-]$

Abstract

here comes an abstract

1 Introduction

Air separation technology, or – more generally speaking – gas separation technology, lies at the heart of the modern process industry. Highly pure oxygen and nitrogen ore uses in many industrial applications. Modern power generation processes, such as the currently developed OXICOAL process, rely on incineration with pure oxygen to produce flue gases with very high carbon dioxide content for further storage. Nitrogen is essential to many widely used processes such as the production of ammonia in the Haber-Bosch synthesis, as fertilizer or in many organic reactions.

The papaer followin this introduction is structured as follws....

Figure 1.1: Demand for industrial gases. []

2 Air separation technology

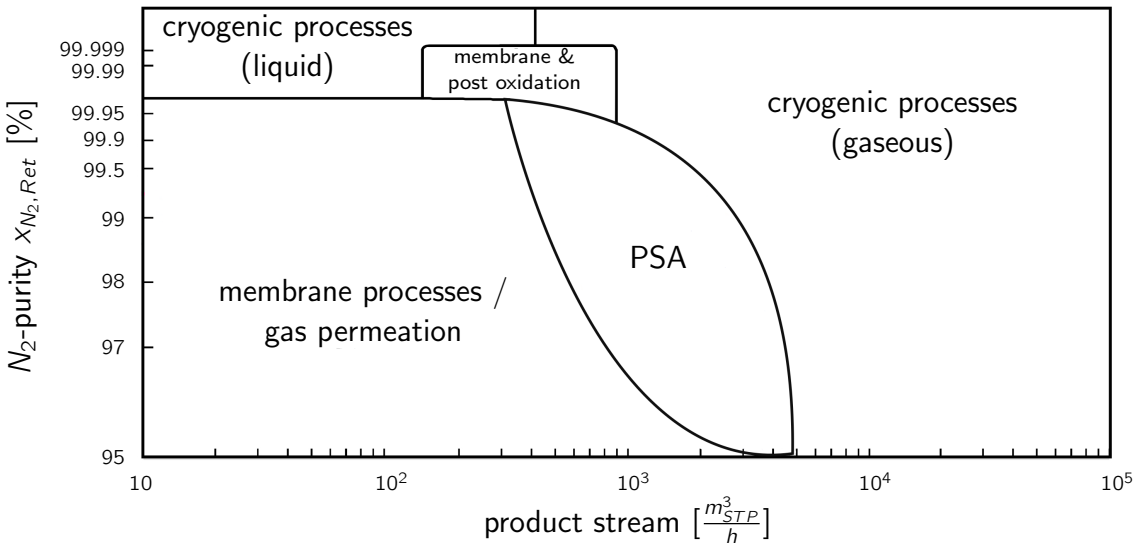

Figure 2.1: Comparison of Air Separation Technologies [21].

There are several ways besides cryogenic air separation that can be employed to separate gas mixtures. In this chapter different competing technologies and their main applications will be discussed. The predominately used technologies are cryogenic distillation, pressure swing adsorption (PSA) as well as gas permeation (GP). In the distillation process the gas is first liquefied. Separation is the achieved by the different concentration differences in vapor and liquid phase. PSA relies on the different affinities of gaseous species to adsorb to certain materials in order to extract a component form a mixture. During gas permeation membranes are used. Each species migrates in different quantities through a given membrane depending on process parameters and membrane structure.

fig. 2.1 illustrates the most economically viable processes depending on product purity and product stream volume. It can be seen that alternative air separation processes cannot supply the high quality or quantity of the cryogenic process. Due to that cryogenic air separation is thought to be the main supplier of highly pure gases in industrial quantities for years to come [7]. The alternative processes however offer some very appealing characteristics, which make them the favorable choice when lower quantities of product or more moderate purity is required. The cryogenic process is always connected with an considerable energy consumption for the liquefaction and compression. Due to that smaller implementations of the process a very unlikely to yield economically sound solutions to a separation problem.

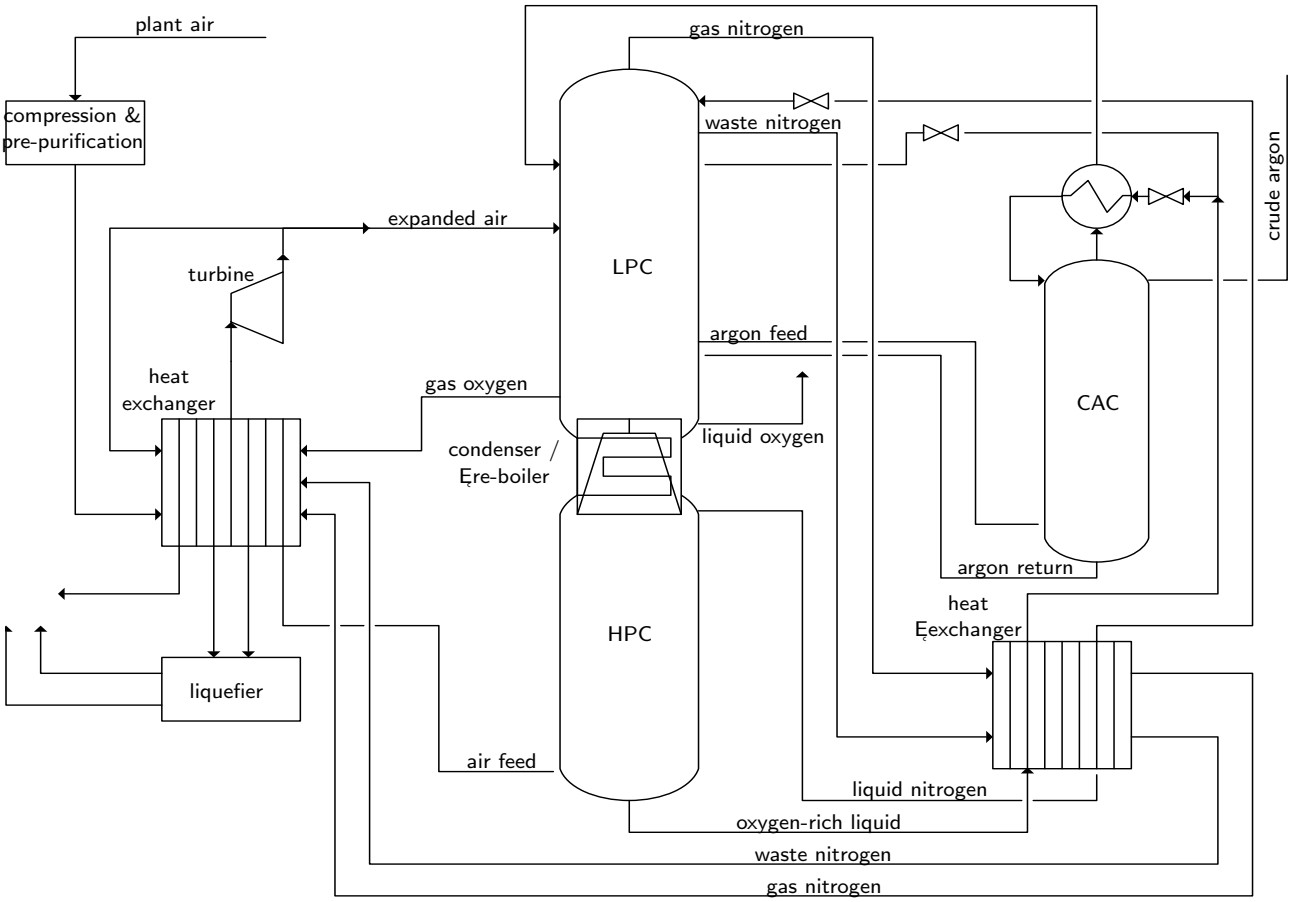

Figure 2.2: Schematic representation of the cryogenic air separation process.

2.1 Cryogenic air separation

Cryogenic Air Separation finds applications over a great variety of industries among others refining, petrochemicals, medical, food & beverages and environmental [24]. Furthermore prospective processes for power generation from fossil sources in form of the integrated gaseous combined cycle (IGCC) integrates the air separation process in order to enable more environmentally friendly power generation [18].

As can be seen in fig. 2.2 double effect heat integrated distillation column lies at the heart of the air liquefaction processes. It consists of a high pressure column (HPC) operating at 0.68 MPa and temperatures below 130 K as well as a low pressure column (LPC) which operates at around 0.13 MPa an comparable temperatures. In order to also attain highly pure argon as a product the process may also include a crude argon column (CAC) which works at slightly lower pressures than the LPC.

The plant air entering the process is initially purified, where carbon and nitrogen oxides as well as solid contaminants are removed, and then compressed to process conditions. The compressed air is then cooled against product streams namely liquefied nitrogen, oxygen and argon. The air stream is then divided into several sub-streams. One of those is fed into the HPC bottom, while another is expanded by means of a turbine and further cooled down through the Joule- Thompson effect. Aside from further cooling energy from the initial compression is thus partially recovered. This expanded air stream is then fed into the LPC. At the bottom of the LPC liquid as well as gaseous oxygen are

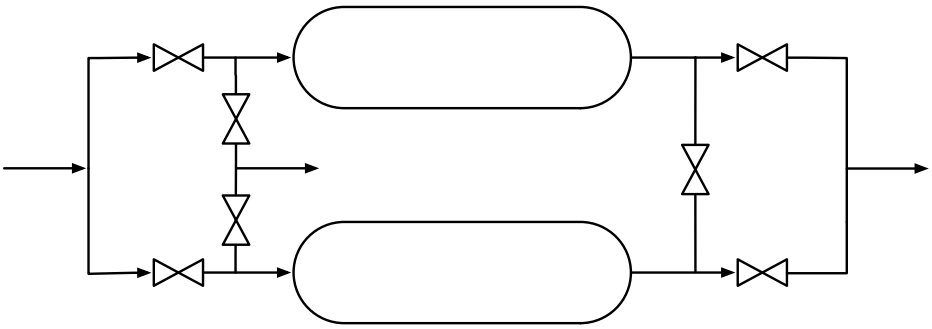

Figure 2.3: Schematic representation of the PSA process.

recovered as desired products. The bottom and top streams from the HPC are made up of an oxygen rich liquid as well as liquid nitrogen. The liquid nitrogen stream is led though an heat exchanger an the fed as reflux into the top of the LPC. The bottom stream is, after heat integration, partially fed into the LPC as well as CAC. From the lower part of the LPC a side stream is drawn and led into the bottom of the CAC. At the same point the reflux from the CAC is fed back into the LPC [27].

2.2 Pressure swing adsorption

Pressure Swing Adsorption has been employed to separate gaseous mixtures for some time. During the 80's and 90's commercial applications for the production of oxygen or nitrogen have gained more and more attention. Especially the ability to construct very compact units the size of a briefcase, have led to the implementation of PSA processes for treatment of asthma patients or other medical appliances. But also larger scale plants have successfully been utilized, for example in the paper industry during the de-lignation of pulp. It remains true however, that for large scale industrial settings with high product quality demands, cryogenic separation remains the most viable alternative.

Separation is achieved during the PSA process by adsorption of one component in the mixture to a given bed. Once the bed is saturated with a the adsorbing species, it has to be regenerated in order to continue production. The ability to adsorb a certain species is dependent on the system pressure. At higher pressures more gas can be adsorbed then at lower pressures. Thus by reducing the pressure in the reaction vessel, the Adsorbent can be regenerated.

In order to avoid non-continuous processes, two or more reaction vessels are employed. Therefore the saturated vessel can be regenerated, while the other one continues production. By alternating adsorption and regenerating in the different vessels continuous production can be achieved. A schematic for a simple two bed cycle is shown in fig. 2.3. Ambient air is first led through the first reaction vessel at the elevated pressure. Within the vessel nitrogen is adsorbed until saturation is reached. At that point the ambient air is led through the second vessel. A fraction of the product stream is fed into the first vessel and used as sweep for the regeneration of the adsorbent at lower pressure.

Depending on the size of the process two different pressure level are used. One cycle adsorbs the nitrogen at a pressure of approximately 7.5 bar while regeneration is done at ambient pressure. Within

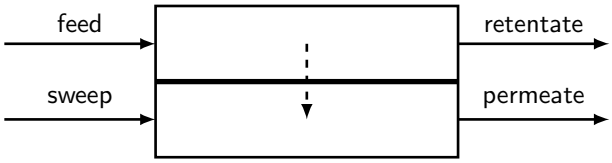

Figure 2.4: Membrane unit for gas permeation.

the alternative approach adsorption occurs under ambient condition, while for the regeneration step a vacuum pump reduces the vessel pressure. This process is the called Vacuum Pressure Swing Adsorption (VPSA).

An important role when designing the product is the choice of the adsorbent. For almost all current applications of PSA alumosilicates or zeolithes have been designed, tailored to the specific separation task. Their main advantages include a high selectivity towards a specic gas to be adsorbed as well as a very homogenous distribution of diameters in the molecular sieve.

2.3 Gas permeation

The separation of mixed gases by membrane process is called gas permeation. Its main strength in comparison with alternative processes are the low energy consumption and the possibility to produce flexible mobile units. As mentioned before it is not however capable of producing high quantity highly pure product streams. As fig. 2.1 illustrates the main application for the gas permeation process are small to moderate product streams at intermediate purities.

fig. 2.4 shows the schematic for a single stage membrane unit. Within the feed stream the gaseous mixture is fed into the unit, which can quickly be implemented. Within the unit one or more species migrate favorably through the membrane. In this case mostly dense polymer membranes are employed used. There have been some impressive results with metallic membranes, but due to the very high material costs they have not been adapted by the industry. Furthermore, since gaseous phases often have rather small molecular species, porous membranes cannot achieve desired separation. The driving force the separation process is a difference in partial pressure or species activity across the membrane. According to the molecular structure of each species, the structure of the separating membrane as well as the process parameters pressure and temperature, they permeate through the membrane in different quantities.

The process of permeation can be subdivided into three separate steps. Sorption at the membrane / feed interface, diffusion through the mostly dense polymer membrane and finally desorption at the permeate side of the membrane.

2.4 Hybrid processes

The three different alternatives presented before constitute the major technologies for separations of gases and therefore the production of pure nitrogen and oxygen. All technologies have their

specific advantages and disadvantages. As the separation of gases remains a major issue when facing upcoming challenges for our industries substantial efforts are being made to improve current processes in terms of ecological and economic performance. A very promising way to achieve such improvements to combine these technologies to form hybrid processes. Membranes offer many favourable characteristics are however rather limited when it comes to large flow-rates and high purities. When lower purities are required or the flow-rates are limited they offer however an efficient and cost effective way for gas separation. Therefore in the past years several alternatives for PSA - membrane [2] or membrane-cryogenic distillation processes [25] have been studied. The membrane can function within the process either as a pretreatment step, where an product enriched stream at medium purities and high flow-rates is produced, or after the main separation, when the main byproducts are already removed, as a last stage to reach very high purities.

3 Process economics

Aside from question wether a certain process is capable of producing products according to its specifications, it needs to be investigated if it does so in an economically viable manner. The modeling of process economics is a powerful tool to estimate project profitability. The evaluation of process economics has three major aims in the design phase.

- Compare design options with regard to profitability.
- Economically optimize a given design.
- Estimate project profitability

In any case the total cost of the project as well as the cash flow structure will have to be analyzed to supply an accurate estimate of the economic conditions. Furthermore an adequate measure to compare and analyze a project in economic terms needs to be employed.

The following sections will first describe how to estimate the total project cost in different stages of the design process. It is evident that, as the more information about a given process becomes available, the accuracy of any cost estimate will increase as well. During the design phase of a process roughly three different stages of cost estimation can be formulated.

- An estimate before designing the process yields an order of magnitude estimation for supporting market research efforts. Error $> 30\%$
- Estimate in the early design phase based on essential process equipment. Error $\pm 30\%$
- Estimate based on an advanced flowsheet and relevant process parameters. Error $\pm 20\%$

Once detail engineering commences, even more accurate calculations with errors reducing to $\pm 5\%$ can be undertaken[20]. At that point a concrete process option will have to be chosen and the investment decision will already have to be made. All optimization measures within the scope of this thesis will have concluded at that time.

Within sec. 3.1 first we will take a look at how the total cost of a chemical process might be estimated at different design stages. Subsequently in sec. 3.2 the different ways of evaluating a certain investment options and estimating a projects profitability will be discussed.

3.1 Project cost

An important factor in every given project is the total cost. During the design of a chemical process many important aspects of the future cost structure are unknown, as the final design is in development.

In general the total cost of implementing and operating a production site can be broken down into several subcategories.

- Battery limit investment
- Utility investment
- Off-Site investment
- Engineering fees
- Working capital

3.1.1 Before process design

Before any details about the process to be implemented are known, an estimate can only give an order of magnitude towards cost to be expected. The cost of the new process C_P can be related to the cost of a reference process C_P^0 by

$$C_P = C_P^0 \cdot \left(\frac{Q_P}{Q_P^0} \right)^x . \tag{3.1}$$

The degression coefficient x needs to be correlated from historical data.

As the overall price structure will change over time, the reference price will not reflect the current market situation. In order to adjust for that shortcoming several price indices are published all over the word. Some of those tailor to special branches of the industry, others give a picture of the price-development in a economy as a whole. The price ration of the prices at different times will then be equal to the ration of the price indices at the respective times

$$\frac{C_1}{C_2} = \frac{I_1}{I_2}. \tag{3.2}$$

For each index an somewhat arbitrary reference year is chosen. Among the most common indices are the Marshall & Swift index, the Nellson-Farrar-Index or the Chemical Engineering index. Some exemplary values for these indices are given in tab. 3.1. As one can see the development within the process industry very well matches the development in the economy as a whole, which is why for this rough estimate general indices should suffice.

3.1.2 During process design

Once the future design has been has been broken down to fewer potential options and first process flowsheets are available a more elaborate approach becomes possible.

	Marshall & Swift Equipment Index 1926 ≡ 100		Nelson-Farrar Refinery Construction Index 1946 ≡ 100	Chemical Engineering Plant Cost Index 1957 ≡ 100
year	all industries	process industry		
1975	444	452	576	182
1980	560	675	823	261
1985	790	813	1074	325
1990	915	935	1226	358
1995	1027	1037	1392	381
2000	1089	1103	1542	394
2001	1093	1107	1565	396

Table 3.1: Price indices and their development.

Battery limit investment

The battery limit investment denotes all investments necessary to have all required equipment for process operations installed on-site. This includes structures necessary to house the process as well as delivery and installation of all individual assets. One major part of these cost will the the process equipment. As the exact manufacturers and models of the equipment will not be known in early design stages, an approach similar to the one in sec. 3.1.1 still needs to be employed. In contrast to before now the cost for individual pieces of process equipment will be considered separately. Each piece of equipment will have an specific feature that most influences its cost. For vessels and reactors this might be volume, while for heat exchangers the required heat exchange area is essential. The price for an piece of equipment i C_E^i can again be approximated by a simple power law

$$C_E^i = C_B^i \left(\frac{Q_E^i}{Q_B^i} \right)^{M^i} . \tag{3.3}$$

A reference price C_B^i is multiplied by the determining quantity Q^i normalized to a reference state Q_B^i and raised to the power M^i specific to each piece of equipment. Reference prices and quantities for various installations can be obtained from literature.

If information on the process conditions are available, they also can be considered in price calculations. Aside from the mere size of the equipment the process conditions will also have an affect on the expected cost. The predominant factors to that respect are pressure, temperature and the question wether corrosive or reactive media, which will require more resistant materials, will be present. Furthermore if a more detailed choice of process equipment is known this is considered as well. For example an plate-fin heat exchanger might be more expensive than a tubular model with the same heat-exchange area. In order to account for all those effect a form factor f_F is applied to the equipment cost

$$C_E^i = C_B^i \left(\frac{Q_E^i}{Q_B^i} \right)^{M^i} f_F^i = C_B^i \left(\frac{Q_E^i}{Q_B^i} \right)^{M^i} \underbrace{\left(1 + f_C^i + f_M^i + f_P^i + f_T^i\right)}_{=f_F^i} . \tag{3.4}$$

Where f_F denotes the form factor, f_C corrects for design complexity, f_M for material selection, f_P adjusts for extreme pressures and f_T for temperature.

As in the previous section all reference prices need to be corrected to compensate for the temporal price development, Here again the already discussed indices are used. Furthermore can regional changes in price structures be considered. Here again have correction factors to prices in an reference region in the world (e.g. USA) been published.

In addition to the purchased cost, the costs for installing the process equipment have an significant effect on the total needed investment of the process. These installation costs include:

- Installations costs
- Piping ,valves and electrical wiring
- Control system
- Structures and foundations
- Insulation and fire proofing
- Labour fees

Those again can be expressed as correction factors to the equipment price. Depending on the status of the information available they can be expressed as one unified factor or broken down to each specific category. One however needs to bare in mind, that costs for piping and valves – pieces of equipment in direct contact with process media – will be affected by the process conditions in a similar way as the actual equipment, whereas the other categories are more likely to remain unchanged. Thus attention needs to be paid, in with fashion the factors will be applied.

A word should be said to the cost for the control system. Most obtainable data will most likely refer to a decentralized control system, as it has been in use for many years. WIth ever more powerful computers a centralized approach, namely model predictive control (MPC) is becoming more relevant. As the structure for such a control system may vary significantly from the common designs, the cost factors may as well.

Services

The utility investments and off-site investments are often referred to as services. Therein included are all measures necessary to supply the process with the media required for operations. This includes but is not limited to generation and distribution of energy, steam, process gases. The utility investments in this context refer to all investments within the greater production site but out of the battery limits of the process. Off-site investments contain everything not contained in the site such as roads, power cables, communication systems or waste disposal. All these costs are expressed as fractions of the equipment cost at moderate temperature and pressure. This means, when applying these fractions, the factors f_M, f_P and f_T should not be considered at this point.

Once again in early design stages one has to resort to factors derived for statistical data, to calculate the cost of raw materials, energy and support media such as lubricants, heat or catalysts. If more detailed information on process streams is available the approach should be refined.

The cost of raw materials C_{RM} can then be calculated if the streams of individual raw materials m_i as well as their specific cost are known.

$$C_{RM} = \left(\sum_{i}^{N_{RM}} \dot{m}_i \cdot C_{RM}^{i} \right) \cdot t_{op}. \tag{3.5}$$

Much in the same way the cost for energy can be calculated. This is once more done for each individual pice of equipment, rather then for the whole process as it has been done for the raw materials. Hence with the needed energy for equipment i with respect to energy carrier j e_{ij} along with the price for energy carrier j C_{EC}^{j} the total energy cost C_{EC} can be assessed.

$$C_{EC} = \left(\sum_{i}^{N_E} \sum_{j}^{N_{EC}} \dot{e}_{ij} \cdot C_{EC}^{i} \right) \cdot t_{op}. \tag{3.6}$$

Working capital

The working capital includes all investments necessary for process operations. This means raw materials, payroll, extended credit to customers and so on. In contrast to all other costs the working capital can partially be retrieved when the process stops operations. How different types of cash flows, extended or owed credit should be handled will be disused in sec. 3.2. In addition to the cost of raw materials needed during process operations, which generate a product stream, raw materials are also needed to fill all vessels, reactors, columns and piping that male up the process. The cost of these needs to be considered as investment and not as operation cost, since more or less the same amount will remain bound until the process seizes operations and it can (partially) be retrieved.

$$C_{FILL} = \sum_{i}^{N_{RM}} V_i \cdot C_{RM}^{i}. \tag{3.7}$$

Total investment

When all contributions to the total investment are considered an estimate for the total price of the process can be calculated

$$C_P = \sum_{i}^{N_E} \left[C_B^i \left(\frac{Q^i}{Q_B^i} \right)^{M^i} \left(f_F \cdot f_{PIPE} + \sum_j f_j \right) \right] + C_{RM} + C_{EC} + C_{FILL} \tag{3.8}$$

It should be emphasized that in early design stages these calculations will at best yield an order of magnitude estimate for the expected cost of implementing a chemical process. Most literature sources give an accuracy of $\pm 30\%$ [20]. As the poject progresses more and more information becomes available an a more accurate estimate can be prepared. Those often rely on actual proposals from prospective manufacturers and suppliers.

3.2 Investment criteria

The total cost of a project its a very important measure to decide wether to undergo a certain endeavor. However in a complex financial system it cannot be taken as the sole factor to compare investment alternatives. Different other indices are used to measure the attractiveness of an investment. One main distinction can be made between different measurements. Those that work with averaged cash flows and consider the project as a singe time periods (sec. 3.2.1) and models that take into account cash flows made at different points in time – so called multi-period models (sec. 3.2.2).

3.2.1 Single period estimation methods

Among the most prominent single period methods are the payout time (POT) and the return of investment (ROI).

Payout time

Payout or amortization time is the time necessary to earn the total investment of the process. It is also often referred to as the break even point. A profitable venture will form that point on begin to make money. A shorter payback time is a measure for an more attractive investment.

$$POT = \frac{\text{capital expenditure}}{\text{incoming cash flow / period}} \tag{3.9}$$

Return of investment

The return of investment is defined as

$$ROI = \frac{\text{average return / period}}{\text{capital expenditure}} \cdot 100\%. \tag{3.10}$$

It denotes the equivalent to an interest rate if the earned interest is not reinvested such that the same Investment is considered in every period. The average return is calculated form the expected returns over certain duration of time. The time considered might either be the total lifecycle of the process or the expected write-off time. As capital expenditure most likely the total investment will be used. However it might give a more precise picture if write-off or the time of individual payments is considered when evaluating the capital expenditure.

3.2.2 Multi period estimation methods

As discussed earlier, when using only averaged values and considering only one time period, a distorted picture of the financial situation will evolve. The source of the money to be invested play a critical role in the evaluation process. Cash reserves, loans, preferred stock or other financial instruments are all viable sources of investment capital. Often a mixture of many different sources is used to allocate

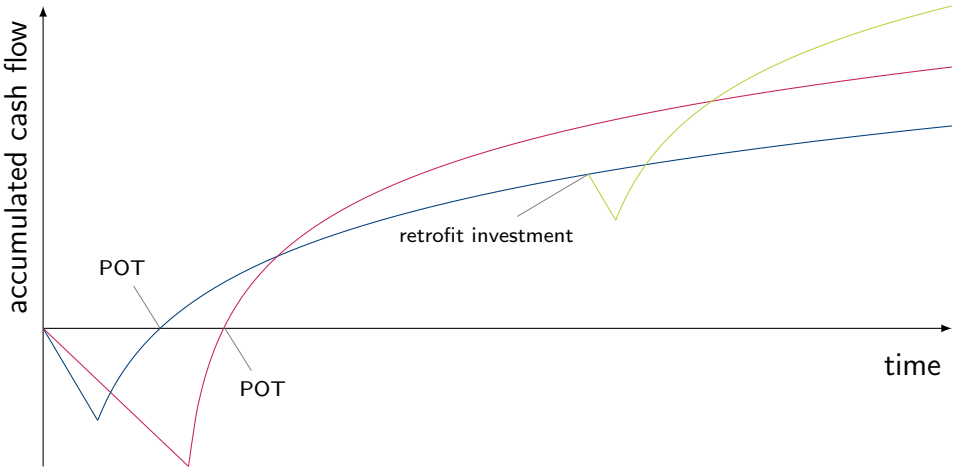

Figure 3.1: Accumulated cash flows over project life cycle.
labelfig:CashFlow

all necessary funds. A generic structure of the cash-flows during the life-cycle of a given project is shown in fig. **??**. When the project commences no revenue is generated and only investments are made. As process operations begin revenue is generated and the slope of the accumulated cash flow curve switches to an upward directions – assuming the project is profitable. As time progresses the produced product might reduce in value through competitors entering the market or other factors. When the curve intersects the abscissa the project investment is earned and the break point is reached. The two investment alternatives highlight that the amount of initial investment will affect the expected revenue. As more information is gathered during operations, opportunities may arise to optimize the process and leverage so far dormant potentials. These so called retrofit Investments would ideally lead to an improved cash flow structure as indicated by the green line.

Before further investigating multi-period model some basic ideas about financial mathematics and the treatment of interest should be reviewed. When investing the capital C_0 at compounded interest for n years at a rate of i %, the compound amount will yield

$$C_n = C_0 \cdot q^n. \tag{3.11}$$

Where q denotes the interest factor

$$q = 1 + \frac{i}{100}. \tag{3.12}$$

On the other hand the current value of an investment that will yield C_n in n years can be calculated by

$$C_0 = C_n \cdot q^{-n} \tag{3.13}$$

The above considerations always assume a single payment at the beginning or end of the entire period. Annuities however are usually in several trances with regular payments to be made or received at predefined instances. Assuming those payments are of equal size a, the final value can be computed by

$$C_n = a \cdot q^{\alpha} \cdot \frac{q^n - 1}{q - 1}, \tag{3.14}$$

while the current value of an annuity yields

$$C_0 = a \cdot q^{\alpha-n} \cdot \frac{q^n - 1}{q - 1}, \tag{3.15}$$

The factor α in the previous equations denotes wether payments are made at the beginning of a period ($\alpha = 1$ or at the end ($\alpha = 0$)

With that multi-period model can be discussed. Here not only different alternatives can be compared, but also the profitability in comparison with investments in financial products can be assessed.

Net present value

The net present value (NPV) describes the amount of money to be invested if all cash flows – incoming and outgoing – are discounted to the project start ($t = 0$). The present value of all expenses is then

$$C_{0e} = e_0 + e_1 \cdot q^{-1} + \cdots + e_n \cdot q^{-n} = \sum_i^n e_i \cdot q^{-i}. \tag{3.16}$$

Here it is given that all expenses are paid at the beginning of each period, as it is the most common case. If revenues r_i are realized then as well an equivalent formula would be attained. In most cases revenues will come in at the end of a period in which case the present value becomes

$$C_{0r} = r_0 \cdot q^{-1} + r_1 \cdot q^{-2} + \cdots + r_n \cdot q^{-(n+1)} = \sum_i^n r_i \cdot q^{-(i+1)}. \tag{3.17}$$

The NPV of a given project is then derived from the present values of all expenses and revenues

$$NPV = C_{0r} - C_{0e}. \tag{3.18}$$

For any project to be considered as investment alternative the present value needs to be positive since otherwise the investment would yield losses.

Discounted cash flow rate of return

The formula for the discounted cash flow rate of return is very similar to the one for a net present value. The difference is, that rather then computing the net present value with given interest rates, the present value is set to zero and the resulting interest rate its then calculated. Other than with the previous methods no analytical solution can be presented but rather an iterative approach to find a solution to

$$0 = \sum_i^n (r_i - e_i) \cdot q^{-i}. \tag{3.19}$$

Here its was assumed that all payments – incoming and outgoing – are made at the beginning of a period. The only variable is the interest rate which is included in the interest factors q. This methods gives the interest rate which would be necessary to earn all time dependent expenses within n years. In this case a higher $DCFRR$ indicates a more attractive investment.

Annuity method

Within the annuity method two different annuities are calculated and then compared. First the annuity a of an investment of C_0 at market conditions is of interest.

$$a = C_0 \cdot \frac{q^{n-\alpha}(q-1)}{q^n - 1} \tag{3.20}$$

This annuity is the amount that could be paid out each period if C_0 is invested, compound interest is considered and all funds are used up at the end of n years.

This is then compared to the annuity of the considered project

$$a_P = \sum_i^n (r_i - e_i) \cdot q^{-i} \cdot \frac{q^{n-\alpha}(q-1)}{q^n - 1}. \tag{3.21}$$

Only if $a_P > a$ is the project more profitable than simply investing the required capital in an financial product.

Interest Rates

With all the presented models its was implicitly assumed that interest rates for debit and credit are equal. The reality however is much different. It will therefore be prudent to use different rates of interest for each case. The basic calculations however remain unchanged. Especially the interest rate that can be earned when investing a certain amount will need to be estimated. As certain products with a know ROI will not necessarily be the most attractive options on the capital market. Thus in many companies there is an internal value given for this interest rate, which is calculated from historical data.

4 Mathematical process model

This chapter deals with the different aspects of the process model developed within the scope of this thesis. As depicted in fig. 4.1 In the case of cryogenic air separation three main tasks for the process can be identified. These are the compression of raw materials, heat exchange with product streams and the separation of air. While those different stages are highly interdependent they will be discussed separately and mathematical models for the main process units will be presented.

The first section (sec. 4.1) deals with a steady state version of the process model. Especially for steady state models the issue of initializing the variables in such a way that the solver can converge to a solution becomes crucial. With that in mind the strategies developed to initialize in particular the distillation columns will be elaborated upon within that first section as well.

The second section (sec. 4.2) is devoted to a dynamic version of the models for some process units. In addition to the models themselves several aspects which arise, when considering process dynamics will also be part of that section.

In the third section (sec. 4.3) of this chapter takes a closer look at how the economics of the process can be captured during process simulation. Understandably, the issue of economic evaluation is closely tied to the sizing of each process unit and with that also to the operational boundaries of the process equipment. As these aspects are for the most part treated uniformly for the steady state case and dynamic case the will be dealt with in a single section.

All presented models have been implemented in the equation based process simulator gPROMS®. Certain aspects arising when implementing the models will be discussed in the last section of this chapter sec. 4.5.

4.1 Steady - state unit models

4.1.1 Separation

Distillation columns are among the most widely studied pieces of process equipment. While much has been accomplished, the robust simulation poses great challenges to this day. In the context of

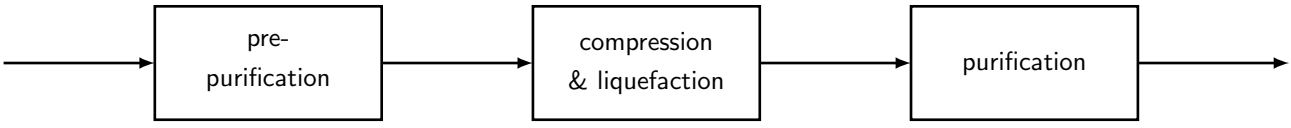

Figure 4.1: simplified cryogenic air separation process.

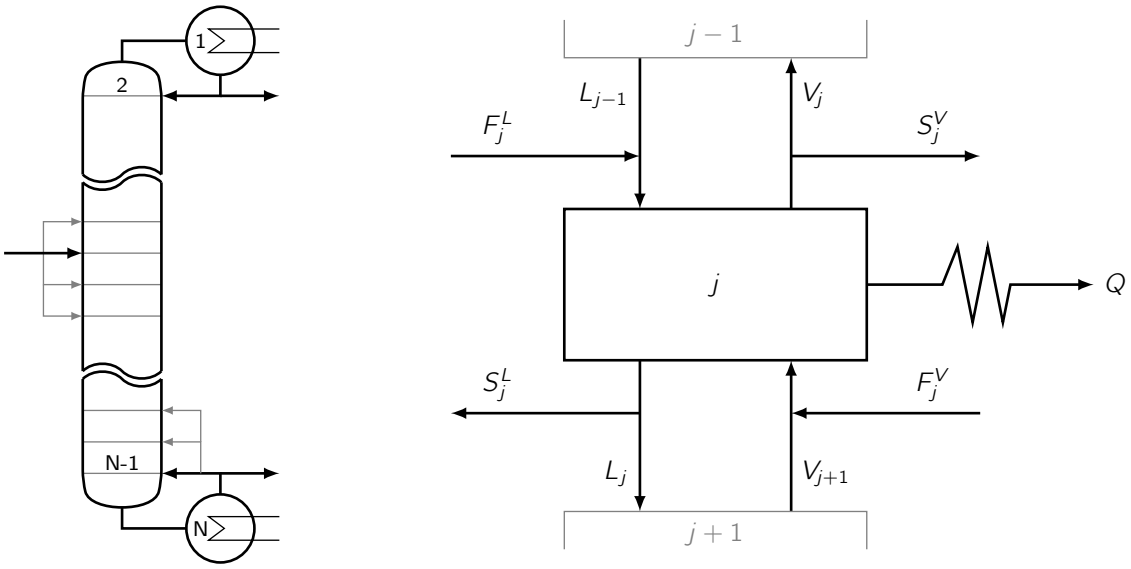

(a) column super structure.

(b) stage super structure.

Figure 4.2: superstructures for column and column stages.

cryogenic air separation the associated mixture displays only moderate non-idealities and furthermore is a zeotropic one. However further complexity is added due to the strong interdependencies of the different columns arising from thermal and material coupling within the process.

In this section first the mathematical formulation for a general steady-state distillation column model will be presented (sec. 4.1.1). The

Distillation column model

In this section the working equations used to model the different distillation columns in the process, known as the MESH equations, are given. These equations, although rather plain at first glimpse, form a set of highly non-linear, highly coupled equations. The solutions of these equations is not a trivial task for current solution algorithms, whose success is highly dependent on the quality of initial guesses provided. Therefore a strategy used for the automated generation of such guesses will be described as well.

The model presented here is not only to be used for the simulation of of a given process, but rather for optimization purposes as well. While several of the continuous decision variables associated whit process optimization can be optimized from a generic set of equations, others need further consideration. The optimization decision which adds the greatest complexity for distillation columns ist the number of trays used in a given separation process. This introduces integer decisions into the model and requires development of a super structure to be used.

The starting point for the modeling a distillation column is considering a single separation stage within the column with all possible connections. Fig. 4.2a shows the superstructure to be used for the complete column, while fig. 4.2b shows a super structure for a singe stage.

As mentioned before the governing equations for a distillation column a known as MESH equations. The acronym MESH stands for material, equilibrium, summation and enthalpy. The corresponding

equations are as follows. If not stated otherwise, all equations presented in this section are true for all stages. In order to improve readability the indices denoting a stage are omitted, if not essential for the meaning of a given equation. For all equations the number of stages in the process is denoted by n_S, while n_C stands for the number of components.

Material balances in their most general form for an inner column stage can be written as

$$0 = \left(V_j + S_j^V\right) \cdot y_{i,j} + \left(L_j + S_j^L\right) \cdot x_{i,j} - V_{j+1} \cdot y_{i,j+1} - L_{j-1} \cdot x_{i,j-1} \\ - F_j^V \cdot z_{i,j}^V - F_j^L \cdot z_{i,j}^L, \qquad i = 1 \ldots n_C \quad j = 1 \ldots n_S. \tag{4.1}$$

Here the vapour F_j^V and liquid F_j^L phase of the feed to the stage j are considered separately. While this is not strictly necessary is allows for certain freedoms in terms of modelling column operations, as sometimes the vapour fraction of a given feed is actually fed into the vapour phase of a stage and therefore effectively in the liquid phase of the stage above.

A certain amount of the liquid or vapour leaving a stage can be withdrawn from the column by means of the vapour S_j^V and liquid S_j^L side draw streams. However it is convenient and seemed to facilitate convergence to define the side draws in terms of dimensionless fractions by relating them to the respective vapour or liquid stream leaving the stage

$$s_j^V = \frac{S_j^V}{V_j}, \qquad j = 1 \ldots n_S, \tag{4.2}$$

$$s_j^L = \frac{S_j^L}{V_j}, \qquad j = 1 \ldots n_S. \tag{4.3}$$

By considering these dimensionless the vapour s_j^V and liquid s_j^L side draws the material balance can be rewritten as

$$0 = \left(1 + s_j^V\right) \cdot V_j \cdot y_{i,j} + \left(1 + s_j^L\right) \cdot L_j \cdot x_{i,j} - V_{j+1} \cdot y_{i,j+1} - L_{j-1} \cdot x_{i,j-1} \\ - F_j^V \cdot z_{i,j}^V - F_j^L \cdot z_{i,j}^L, \qquad i = 1 \ldots n_C \quad j = 1 \ldots n_S. \tag{4.4}$$

As the model is also to be used for optimization purposes further extensions are necessary. The location of individual feeds as well as the number of theoretical or real stages of the column is to be optimized. To accommodate that need, new variables are need, namely the feed split ζ_{ij}^F for feed i to stage j as employed by [10] are introduced. The split variables are integer variables that can take a value of either 0 or 1. Additionally it is assumed that each feed will only be fed to a single stage thus

$$1 = \sum_{j=1}^{N} \zeta_{ij}, \qquad i = 1 \ldots n_F, \quad j = 1 \ldots n_S, \tag{4.5}$$

where n_F denotes the number of feeds, comprised of vapour (F^V) and liquid F^L feeds.

In order to optimize the number of stages several superstructures are possible. One can optimize the reboiler reflux location and condenser reflux location or each single one along with the feed and side draw locations. The stage number is then changed as all stages between condenser or reboiler reflux are effectively rendered inactive. The solution of the mass and energy balances for each respective stages becomes trivial as only one single vapour or liquid stream enters and exits the stage. While the choice if condenser and or reboiler reflux is optimized is somewhat arbitrary some studies have shown [13] that the strategy of optimizing only feed location and reboiler reflux location possesses some numerical advantages in terms of performance of the solution algorithm.

With the newly introduced split variables for liquid ζ_{ij}^{L} and vapour ζ_{ij}^{V} as well as the reboiler reflux ζ_{j}^{R} and the liquid ζ_{ij}^{SL} and vapour ζ_{ij}^{SV} side draws, the material balances can be written as

$$\begin{aligned} 0 = {} & \left(1 + s_j^V\right) \cdot V_j \cdot y_{i,j} + \left(1 + s_j^L\right) \cdot L_j \cdot x_{i,j} - V_{j+1} \cdot y_{i,j+1} \\ & - L_{j-1} \cdot x_{i,j-1} - \sum_{k=1}^{n_F} \zeta_{kj} \cdot F_j^V \cdot z_{i,j}^V - \sum_{l=1}^{n_F} \zeta_{lj} \cdot F_j^L \cdot z_{i,j}^L - \zeta_j^R \cdot V_{n_S} \cdot y_{in_S}, \\ & i = 1 \ldots C, \quad j = 1 \ldots n_S, \quad k = 1 \ldots n_F, \quad l = 1 \ldots n_F. \end{aligned} \tag{4.6}$$

Furthermore to be able to optimize side draws, the stripping factors have to be reformulated accordingly

$$s_j^V = \frac{\sum_{i=1}^{S^V} \zeta_{ij}^{SV} S_j^V}{V_j}, \qquad j = 1 \ldots N, \quad i = 1 \ldots S^V, \tag{4.7}$$

$$s_j^V = \frac{\sum_{i=1}^{S^L} \zeta_{ij}^{SL} S_j^L}{L_j}, \qquad j = 1 \ldots N, \quad i = 1 \ldots S^L. \tag{4.8}$$

Equilibrium between a vapour and liquid pase ia achieved when the chemical potentials for each component in the pases are equal. This is commonly expressed by a equilibrium K_i constant. With that the equilibrium equation can be written as

$$y_i^{eq} = K_i \cdot x_i, \qquad i = 1 \ldots n_C. \tag{4.9}$$

The requirement for equal chemical potentials can be expressed in terms of the vapour f_i^V and liquid f_i^L fugacities [3].

$$f_i^V = f_i^L, \qquad i = 1 \ldots n_C. \tag{4.10}$$

This can also be written in terms of the, liquid activity coefficient γ_i, the pointing factor F_{Pi}, the reference vapour fugacity coefficient φ_i, the vapour pressure p_i^S as well as the system pressure p along with the vapour and liquid molar fractions

$$\gamma_i \, F_{Pi} \, \varphi_i^0 \, p_i^S \, x_i = \varphi_i \, p \, y_i, \qquad i = 1 \ldots n_C. \tag{4.11}$$

By reformulating eq. (4.12) an expression for the equilibrium ratios can be derived

$$y_i^{eq} = \underbrace{\frac{\gamma_i \, F_{Pi} \, \varphi_i^0 \, p_i^S}{\varphi_i \, p}}_{K_i} x_i, \qquad i = 1 \dots n_C. \tag{4.12}$$

The equations to determine the quantities used when computing the equilibrium ratios are by themselves functions of temperature, pressure, and vapour as well as liquid molar fractions. They are further discussed in sec. **??**. It therefore becomes evident that the equilibrium ratios are a major source non-linearities in the MESH equations.

When simulating a distillation process one might consider only equilibrium stages. This however will in most cases not reflect the true behaviour of a given stage as the time a vapour and liquid phase are in contact might not be sufficient to achieve equilibrium. This can be accounted for by introducing the Murphee tray efficiency [15]

$$\eta_{ij}^{eq} = \frac{y_{ij} - y_{ij+1}}{y_{ij}^{eq} - y_{ij+1}} \qquad i = 1 \dots n_C \quad j = 1 \dots n_S. \tag{4.13}$$

While several models to approximate these efficiencies have been investigated, their predictions are most often rather poor [9] and their evaluation rather complex. Furthermore as indicated in the formula they might differ for different species involved. For the scope of this model however they are not computed separately, but rather supplied and assumes uniform for each stage and component.

Enthalpy balances are again written considering the previously defined stripping factors and splitting variables

$$\begin{aligned} 0 = {} & \left(1 + s_j^V\right) \cdot V_j \cdot h_j^V + \left(1 + s_j^L\right) \cdot L_j \cdot h_j^L - V_{j+1} \cdot h_{j+1}^V \\ & - L_{j-1} \cdot h_{j-1}^L - \sum_{k=1}^{F^V} \zeta_{kj} \cdot F_k^V \cdot h_j^{FV} - \sum_{l=1}^{F^L} \zeta_{lj} \cdot F_j^L \cdot h_j^{FL} - \zeta_j^R \cdot V_N \cdot h_N^V, \\ & i = 1 \dots C, \quad j = 1 \dots N, \quad k = 1 \dots n_F, \quad l = 1 \dots n_F. \end{aligned} \tag{4.14}$$

Condenser and reboiler are modeled more or less as regular column stages. However they possess certain specialties that are explicitly considered in the column model. For one it is assumed that no feeds enter the reboiler and condenser stage. Furthermore no vapour side stream is drawn from the condenser stage and no liquid side stream from the reboiler stage.

Additionally the condenser stage needs to examined a little further. In terms of operations several assumptions can be made for the condenser. In general one can distinguish a total, partial vapour and partial vapour liquid condenser. For the total condenser all vapour that enters the respective stage

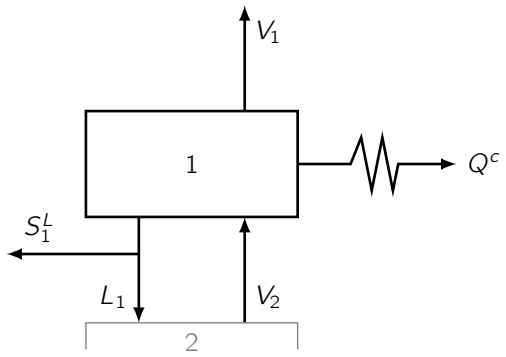

(a) condenser stage.

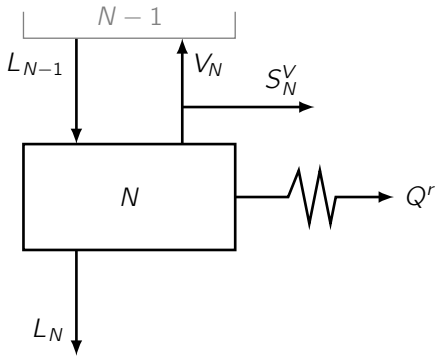

(b) reboiler stage.

is condensed and only liquid product is drawn . The partial vapour condenser condenses only the vapour the is fed back into the column and all product that is drawn is gaseous. The partial vapour liquid condenser denotes the most general case, where part of the incoming vapour is condensed and product is drawn from the vapour and liquid phase. The most important thing to consider in these different cases, is that while in both partial condensers a vapour liquid equilibrium takes place, due to the absence of vapour the same does not hold for the total condenser. To accommodate that fact the MESH equations have to be adjusted [19]. While the material and energy balances remain unchanged the equilibrium equations have to be altered. First the vapour and liquid compositions are set equal for all but one component

$$x_{i1} = y_{i1} \qquad i = 1 \dots C-1, \tag{4.15}$$

and the condenser temperature is determined by the bubble point equation

$$1 = \sum_i K_{i1}(T_1, p_1, x_1, y_1) \cdot x_{i1} \qquad i = 1 \dots n_C. \tag{4.16}$$

When implementing the model in a process simulator it is sensible to consider, that due to the limited accuracy of computers the omitted component in eq. (4.15) needs to a non-trace component in the condenser stage. The implemented model therefore as to specify such a component when a total condenser is chosen to avoid numerical difficulties.

In practice it is highly unlikely, that the exact amount of energy required to condensate all liquid will be drawn from the condenser. More likely, if all vapour is condensed, a little more energy will be withdrawn and slightly sub-cooled liquid will leave the condenser. Therefore the model includes the possibility to specify a degree of sub-cooling T^{sub} which will be considered when calculating bubble point temperature

$$1 = \sum_i K_{i1}(T_1 + T^{sub}, p_1, x_1, y_1) \cdot x_{i1} \qquad i = 1 \dots n_C. \tag{4.17}$$

Pressure along the entire column is often specified in the steady-state case However as it is inconvenient and unpractical to specify a pressure for each stage one might either specify a pressure

at the top and bottom stage and assume a uniform pressure profile along the column, or specify either top p_1 or bottom pressure p_N along with a total pressure drop Δp, or a stage-wise one Δp_{stage}. However the issue is further complicated if one considers the case of optimization for number of trays. In that case several trays will become inactive. For those trays the mass and energy balances become trivial, as only liquid enters and exits these trays. (For the case employed here, where the reboiler reflux is being optimized). This also means, that from the last active tray down to the reboiler – if present – there should be a uniform profile. however, if a uniform pressure profile from that stage down is not enforced, the solver will have to compensate for slight changes in the equilibrium due to pressure variations with minimal vapour flow-rates. This is very undesirable, as it might to lead to severe problems in the solver, or the calculation of other properties, dependent on these values. To account for this issue, the reboiler reflux split can once more be employed

$$p_i = p_{j-1} + \left(1 - \sum_{k=1}^{j-1} \zeta_k^R\right) \cdot \Delta p_{j-1} \qquad j = 1 \dots n_S. \tag{4.18}$$

As an alternative to specifying the pressure, one might consider calculating the pressure drop form (semi)-empirical models. There a numerous correlations for different types of column internals. These correlations become particularly important id column dynamics are to be considered, as they make a connection between holdups and flow-rates within the column. Two different pressure drop models have been implemented, one for trayed columns and another one for structured packings. As they are closely tied to dynamics, they will be discussed in closed detail in sec. **??**.

Specifications & initialization

The equation systems presented above is comprised of NC component balances, NC equilibrium equations, $2N$ summation equations and N energy balances. This gives a total of $N(2C + 3)$ equations. On the other hand there are N temperatures and pressures, $2N$ molar flow rates, N energy streams, and NC vapour as well as and liquid concentrations. Additionally the feed flow rates compositions and temperatures and the side draw split fractions or flow rates appear as variables. The feeds and side draws would usually be specified, which leaves a total of $N(2C + 5)$ variables.

The pressure profile of a distillation column is usually specified. Either by explicitly assigning a given pressure to each stage, or more conveniently by defining a pressure either the top or bottom pressure as well as the pressure drop per stage

$$\Delta p_{stage} = p_i - p_{i-1}, \qquad i = 2 \dots N. \tag{4.19}$$

In terms of unit operations this pressure drop is of high significance, as many columns can only be feasibly operated, if the pressure drop does not exceed certain limits. In case of the ASU the production of Argon only became feasible as structured packings, which display a very low pressure drop, became available. This is due to the large number of theoretical stages required to attain the desired Argon purities.

The energies Q_i denote addition heaters or cooler on the respective stages. For all intermediate stages these values would be specified as well. If all energies would be specified, that would – along

specification	replacement for H_1	replacement for H_N
reflux or boilup ratio	$0 = L_1 - \nu^D \cdot (V_1 + S_1^L)$	$0 = V_N - \nu^R \cdot L_N$
temperature	$0 = T_1 - T_{spec}$	$0 = T_N - T_{spec}$
product flowrate	$0 = (V_1 + S_1^L) - D$	$0 = L_N - B$
component product flowrate		$0 = L_N \cdot x_{iN} - b_i$
mole fraction	$0 = y_{i1} - y_{i,spec}$	$0 = x_{iN} - x_{ispec}$

Table 4.1: discrepancy functions for different column specifications.

with the pressure profile – sum up to $2N$ specifications, which leaves $N(2C + 3)$ unknowns. As the number of equations and unknowns are the equal, this system can then be solved.

In practice it is often challenging to correctly guess the condenser and reboiler heat loads in advance. This is especially true since they have a tremendous impact on the overall performance of the column. Hence it is often desirable to supply other specifications than the respective heat loads. To allow for such specification so called discrepancy functions can be introduced [15], which replace the energy balance for the condenser and / or reboiler stage.

One common specification is the so called reflux ratio $\nu^D = \frac{L_1}{V_1+S_1^L}$ for the condenser, or the boilup ratio $\nu^R = \frac{L_N}{V_N}$ for the reboiler. They are defined as the ratio of the molar flowrate sent back into the column over the product flowrate which leaves the column. For the reboiler this denotes a liquid stream, while for the condenser the product can be gaseous and liquid. Specifying this leads to

$$0 = L_1 - \nu^D \cdot (V_1 + S_1^L), \tag{4.20}$$

$$0 = V_N - \nu^R \cdot L_N, \tag{4.21}$$

as discrepancy functions. I addition to that further specifications are conceivable. Most commonly distillate (D) or bottoms (B) flow rates, or purities, component flow rates (d_i, b_i) or temperatures. The corresponding discrepancy functions are summarized in tab. 4.1.

The specifications for the reboiler stage are quite straightforward, in contrast to that, different cases for the condenser have to be considered. In the most general case the top product can be drawn as vapour and liquid. This case is here called a partial vapour liquid condenser. The other cases are a total condenser, where all the vapour entering the condenser stage is condensed, and all product is drawn as a liquid stream, as well as a partial vapour condenser, where only the reflux is condensed and all product is drawn as vapour. As discussed earlier no VLE takes place in the condenser stage, if a total condenser is specified, which needs to be accounted for. Both the total and partial vapour condensed implicitly include an extra specification since in former case the top vapour product flow rate becomes zero and in the latter the top liquid product flowrate. Furthermore a specification of the condenser energy is infeasible as well as implicitly given for the total condenser. In case of the partial vapour liquid condenser no implicit specification is given, which requires an additional specification. In general two top specifications are necessary, whereas only one bottom specification is required. These top specification can include the condenser duty, any top flowrate, the reflux ratio as well as a newly introduced quantity, the top vapour fraction defined as

$$\nu^{vap} = \frac{V_1}{V_1 + S_1^L}. \tag{4.22}$$

As mentioned before the solution of the MESH equations can pose a considerable problem to numerical solvers. It is therefore necessary to supply the solver with feasible estimates for the involved variables that can be used as an initial guess for convergence of the process model. A lot of effort has been spend to formulate robust strategies to initialize distillation column models. One of the most prominent is the so called Inside-Out algorithm first introduced by Boston and Sullivan [6]. Within this algorithm an inner and outer iterative loop are employed. Within the outer loop approximate parameters for simplified models of phase equilibrium and enthalpy are computed by rigorous thermodynamic models and guesses for stage temperatures and concentrations. Within the inner loop new stage temperatures and concentrations are attained by solving the MESH equations using the simplified thermodynamic models. Once the inner loop converges the simplified model parameters are updated within the outer loop by means of the newly calculated temperatures and concentrations. This algorithm converges in many cases even for very poor initial guesses and has been extended to handle complex columns with side-draws and even reactive distillation [5]. It is still in use in the process simulator Aspen Plus®. However as it is used within an modular algorithmic environment it is not applicable to equation based simulators such as gPROMS®.

More recently other approaches have been published to attain improved initial guesses. Fletcher and Morton [12] proposed the solution of a column model at infinite reflux and zero feed flow rate. This leads to a much simplified model which can be solved more easily. The computed purities and stage numbers can give valuable insight into the process model. As this approach relies on the solution of a simplified model and has no algorithmic elements, it can be implemented in equation based process simulators.

Another strategy that has been successfully applied to zeotropic and azeotropic mixtures relies on solving the column model for the limiting case of the adiabatic column [4]. The adiabatic column in this case is the column with the minimal entropy production in a real column. To avoid entropy production all streams that come in contact must be in equilibrium. To achieve this the column would have to employ an infinite number of stages and have an infinite number of heat exchangers along its length. The adiabatic column then uses only two heat exchanger in the condenser and reboiler stage and assumes a pinch point at the feed stage.

Furthermore a much simpler approach has proven adequate for many applications [15] which is also employed as a starting point in this work. Therein feed properties are used as initial guesses. First a linear temperature profile form the boiling temperature to dew temperature of the combined feed mixture is used to initialize temperatures, whereas a simple flash at average column pressure and feed temperature yields a vapour and liquid concentration which is used as uniform profile for every column stage. However as the feed might be sub-cooled liquid or super-heated vapour, the TP-Flash is replaced by a specified vapour fraction. As vapour fraction for the flash initial estimates of the vapour and liquid flow rates at the top and bottom of the column are used. The stage-wise molar flow-rates are computed from the constant molal overflow assumption, which postulates a constant heat of vaporization and yields therefore uniform liquid and vapour flow-rates within a column section. A section in this case is denoted by any feed location where the flow-rates change due to the added feed. In the feed stages a super heated or sub-cooled feed is also considered by means of an extended vapour fraction

$$q^F = \frac{h^F - h^L}{h^V - h^L}. \tag{4.23}$$

While this approach leads to model convergence in many cases, it is not entirely robust. While the system considered in this case displays only moderate non-idealities it is highly cupeled. Especially the low pressure column (LPC) has multiple feeds and side draws, which leads to non-convergence if the aforementioned initialization strategy is employed. However the fact that the system is not highly non-ideal can be exploited. Whenever the K-values are not too much dependent on mixture composition an intermediate step can be used to refine concentration guesses. The constant molal overflow assumption is retained and the equilibrium ratios are computed based on the initial guesses from the first stage. The component balance is then reformulated only in terms of liquid component flow-rates l_{ij}

$$0 = \left((1 + s_j^V) \cdot K_{ij} \cdot \frac{V_j}{L_j} + (1 + s_j^L)\right) \cdot l_{ij} - \frac{V_{j+1}}{L_{j+1}} \cdot K_{ij+1} \cdot l_{ij+1} - l_{ij-1} \\ - F_j^V \cdot z_{i,j}^V - F_j^L \cdot z_{i,j}^L, \qquad i = 1 \dots n_C \quad j = 1 \dots n_S. \tag{4.24}$$

eq. (4.24) is linear in the liquid component flow rates. Furthermore vapour component flow rates are substituted in the linear component balance and can be computed by

$$v_{ij} = K_{ij} \cdot \frac{V_j}{L_j} \cdot l_{ij} \qquad i = 1 \dots n_C \quad j = 1 \dots n_S. \tag{4.25}$$

On of the reasons eq. (4.24) is formulated in terms of component flow rates rather than molar fractions, is that the molar fraction computed in that manner would not be normalized. If the mole fractions are computed from the component flow rates normalization is implicitly given

$$x_{ij} = \frac{l_{ij}}{\sum_k^C l_{kj}} \qquad i = 1 \dots n_C \quad j = 1 \dots n_S, \tag{4.26}$$

$$y_{ij} = \frac{v_{ij}}{\sum_k^C v_{kj}} \qquad i = 1 \dots n_C \quad j = 1 \dots n_S. \tag{4.27}$$

The total molar flow rates used in eq. (4.24) are computed by solving stage-wise total mass balances under the constant molal overflow assumption. This assumption postulates that the heat of vaporization is independent of system composition. Therefore always the same amount of liquid enters and leaves a given stage

$$0 = L_j + S_j^L - L_{j-1} - (1 + q_F^L) \cdot F_j^L - q_F^V \cdot F_j^V \qquad j = 1 \dots N. \tag{4.28}$$

Only at feed and side draw stages the total flow rates change. To introduce some more accuracy to the model, the available information about the feed is considered. When a feed enters as super-heated

vapour or sub-cooled liquid, it has the capability to evaporate some liquid or liquefy some vapour. To account for that fact the feed energy parameters q_F^L and q_F^V are introduced

$$q_i^{FV} = \frac{H_i^{FV} - H_i^V}{H_i^V - H_i^L}, \qquad i = 1 \dots F^V, \tag{4.29}$$

$$q_i^{FL} = \frac{H_i^{FL} - H_i^L}{H_i^V - H_i^L}, \qquad i = 1 \dots F^L. \tag{4.30}$$

The vapour total flow rates are then computed from the total mass balances

$$0 = L_j + S_j^L + V_j + S_j^V - L_{j-1} - V_{j+1} - F_j^L - F_j^V, \qquad j = 1 \dots N. \tag{4.31}$$

As no energy balances are included at this stage, the condenser and reboiler stage are characterized by the reflux ($\nu^c = \frac{V_1}{L_1}$) or boilup ratio ($\nu^r = \frac{V_N}{L_N}$) respectively. This leads to

$$0 = V_1 - \nu^c \cdot L_1, \tag{4.32}$$

$$0 = L_N - \nu^r \cdot V_N. \tag{4.33}$$

To close the equation system the global mass balance is included

$$0 = V_1 + L_N + \sum_{j=1}^{N} (S_j^V + S_j^L - F_j^V - F_j^L), \qquad j = 1 \dots N. \tag{4.34}$$

For more complex systems more elaborate strategies have been developed, which essentially try to incorporate some of the principals from the inside out algorithm into an equation based environment. The process simulator gPROMS® allows for definition of standardized initialization procedures as well as different model variants that can be solved consecutively. With that strategies were developed that proved successful for more complex mixtures and even three phase systems. As these strategies are closely linked to the implementation in gPROMS® and the programm capabilities, they will be discussed in sec. 4.5

Furthermore ist should be noted, that not all specifications are compatible with the initialization strategies described above. While this issue has been addressed, it also will be explained in the implementation section.

Example To illustrate how the initialization procedure works an example has been constructed of a rather complex column – or column section – with multiple feeds and side draws (fig. 4.2). It is taken from an example process of cryogenic air separation. The column in question is a column section without an condenser stage and displayed the most difficulties in terms of convergence when constructing the process flowsheet.

In addition to the aforemention initialization strategy, columns with side draws present are handled in a slightly different manner. Initially the side draws are disregarded. Then the initialization procedure is carried out. Once the column without side draws has converged, a homotopy approach

$$f(\mathbf{x}) = (1 - \alpha) \cdot f_0(\mathbf{x}) + \alpha \cdot f_1(\mathbf{x}) \tag{4.35}$$

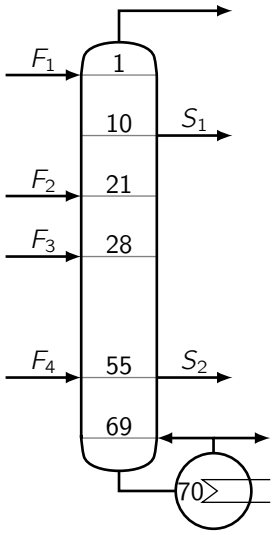

Figure 4.3: example column.

feed specifications

stream	flow $[\frac{kmol}{hr}]$	$z_{O_2}[-]$	$z_{N_2}[-]$	$z_{Ar}[-]$	$T[K]$	$p[bar]$
F_1	2985.77	4.674E-10	0.9999	6.378E-7	79.45	1.3
F_2	1836.36	0.2095	0.7812	0.0093	98.91	1.3
F_3	7609.06	0.2920	0.6950	0.0130	81.88	1.3
F_4	774.94	0.9161	5.393E-12	8.394E-2	92.13	1.8

column specifications

stages	S_1 frac	S_2 frac	boilup ratio	p^{top}	p^{bot}
70	10	0.15	3.5	1.2 bar	1.3 bar

Table 4.2: column specifications.

is employed, where the parameter α is initially set to zero and then gradually moved to a value of one. During the initialization homotopies could generally be employed to move from one step to another. While in some cases robustness is improved by such a strategy, it is always computationally far more expensive then simply jumping between different stages.

For clarity reasons the different steps of the initializations procedure a repeated in a tabular manner

1.
   - linear temperature profile between dew (T^{dew}) and bubble point temperature (T^{bub}) of mixed feed.
   - linear profile between feed flash vapour and liquid compositions for liquid stage compositions.
   - constant profile for vapour compositions.
   - molar flow rates from constant molar overflow model.
   - side draw flow rates set to zero.
2.
   - total molar flow rates form constant molar overflow model.
   - simplified equilibrium ratios from initial liquid mole fractions and linear temperature profile.
   - liquid and vapour mole fractions from linearized mass balances.
3. rigorous solution of MESH equations with side draws still set to zero.
4. homotopic approach to MESH equations with side draws considered.

The resulting profiles for oxygen and nitrogen concentrations in the example column can be seen in fig. 4.4a and fig. 4.4b.

4.1.2 Heat exchange

The issue of heat integration is essential to the economic performance of cryogenic air separation. Foremost one must consider the special column configuration used in the process. Since operation of

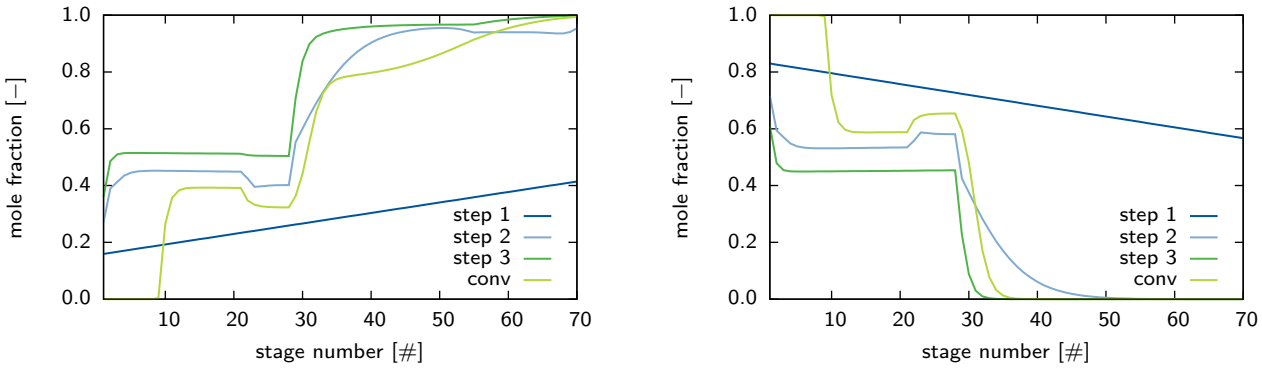

(a) oxygen concentration profiles.

(b) nitrogen concentration profiles.

Figure 4.4: initialization example concentration profiles.

the condenser in the low pressure section only becomes possible if the reboiler in the high pressure section functions as heat sink, no external utilities are supplied to either unit. Rather they are combined into a single heat exchange unit. Thus the absolute value of the reboiler energy must matched by the energy recovered from the condenser. Furthermore the material streams entering the process can – and should – exchange heat with the process streams leaving it. The combined condenser / reboiler for LPC / HPC column is assumed as a given heat exchange. This makes sense insofar, as this is a necessity in terms of the actual physical implementation of the process units. Also the usage of the oxygen rich liquid from the HPC as coolant in the Argon condenser is assumed as fixed.

This leaves the process stream leaving the compression stage of the process as well as all product and waste streams leaving the process. All those streams are – for simulation purposes and also in some process implementations – fed into a single multi-stream heat exchange unit. In actual processes all heat exchange and much of the process operations take place in the so called "cold box". As such a heavily insulated area is referred to. This is done to minimize heat exchange with the surroundings. Therefore and for further reasons compact heat exchange units such as plate-fin multi-stream heat exchangers are favoured when dealing with cryogenic processes in general and the cryogenic air septation in particular.

Due to the importance of heat integration to the ASU process some thought sould be given as to what modelling approach should be employed. Although the field of heat integration is one of the most intensively studied within process engineering, only a limited amount of approaches is available in open literature [16].

Traditionally heat integration has been carried out in a sequential manner, where it is for the purposes of process optimization assumed, that all heating and cooling is done by external utilities. After an (locally) optimal process configuration is identified, all hot and cold streams within the process are identified, and their temperature intervals fixed. In subsequent steps first the minimum utility requirements, and maximum number of heat exchangers are identified, and a specific heat exchange network (HEN) is designed. While this approach has been successfully applied to a multitude of processes and led to substantial savings, it is questionable if such a sequential approach will yield an optimal or near optimal solution.

Therefore some efforts have been made to develop efficient strategies for simultaneous process

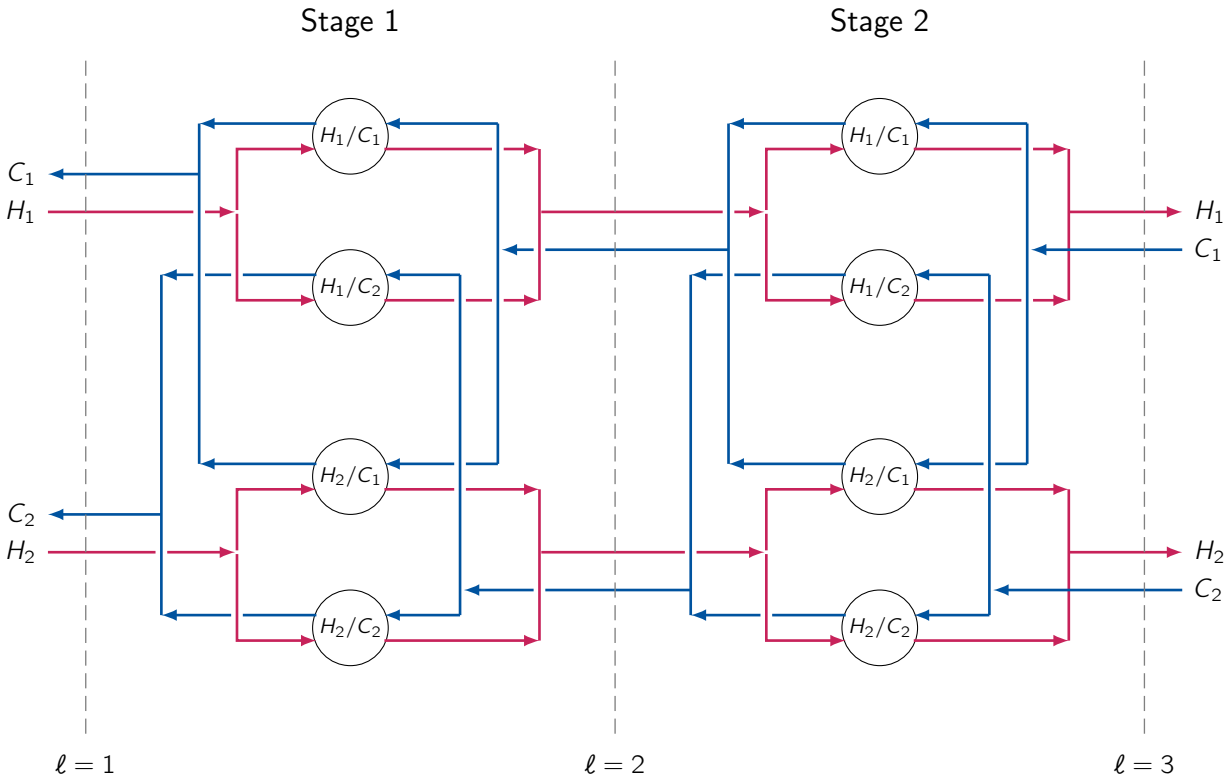

Figure 4.5: Superstructure for multi-stream heat exchanger. [26]

optimization and heat integration. Two general approaches can be distinguished. The first one based on the pinch concept. These methods are able to identify the minimum heat requirement as well as stream temperatures during process optimization. The first model along these lines was published by Duran and Grossmann [11] in 1986. They introduced a limited number of quite well behaved constraints into the optimization model to ensure no minimum driving force violations. Recently this model has been extended to handle phase changes and by fixing the utilities to zero been applied to the design of a multi-stream heat exchanger [16]. The major drawback with these methods is that one cannot target area of a given heat exchanger as the approach temperatures are not computed by the model. Therefore the sometimes substantial trade-off between the cost for heat exchange area and utility cost cannot be regarded.

A second approach employs superstructures of a HEN to find optimal matchings of process streams. No pinch point calculations are required, as the actual heat exchange is more or less modeled explicitly. This leads to the benefit, that approach temperatures as well as exchanged heat duties between each stream coupling are known within the model, and the cost of the designed unit can be considered in an economic objective function.

The approach and respective superstructure adapted in this thesis were first published by Yee and Grossmann [26]. Fig. 4.5 shows the stage wise superstructure for a HEN consisting of two hot and two cold streams.

In this stagewise structure each hot stream can exchange heat with each cold stream within each stage. The following assumptions were made when the model was developed

- Constant heat capacities

- Constant heat transfer coefficients
- Countercurrent heat exchangers
- Isothermal mixing at each stage.

The assumption of constant heat capacities is a common one in the design of HEN's. When no phase boundaries are passed and the temperature range of the involved is not too wide, it is a reasonably good approximation of the real conditions. While constant heat transfer coefficients a re assumed the model leaves the flexibility to define different coefficients for each pairing of hot and cold streams. Countercurrent heat exchangers are common in industrial practice. This assumption however does not really pose a limitation, as the model can easily be altered to account for concurrent units.

The last assumption of isothermal mixing is a more major one. It has been introduced as it allows for significant simplifications and leads to a model, where all constraints are linear and all non-linearities are restricted to the objective function. While that is certainly not true for the entire process model, it should at least allow for some reductions in the model complexity. The assumption states, that regardless of which streams a given stream exchanges heat with, it will leave at the same temperature. Due to that all energy balances around each unit in the superstructure can be eliminated as well as the subsequent mixing of the streams.

Model equations First of all a heat balance at each stage is necessary

$$F_i(T_{i,\ell} - T_{i,\ell+1}) = \sum_j q_{ijk} \tag{4.36}$$

$$f_j(T_{i,\ell} - T_{i,\ell+1}) = \sum_i q_{ijk} \tag{4.37}$$

The heat exchange area A_{hx} can be computed from the exchanged energy, the heat transfer coefficients α_{ij} and the logarithmic mean temperature difference $LMTD$.

$$A_{hx} = \sum_i \sum_j \sum_k \frac{q_{ijk}}{\alpha_{ij} * LMDT_{ijk} + \delta} \tag{4.38}$$

While the small number δ is included to avoid problems in the program, when $LMDT$ becomes zero In order to avoid further numerical difficulties when the approach temperatures ΔT_{ij} at each side of an exchange unit approach zero, it was proposed to use an approximation introduced by Chen [8]

$$LMDT_{ijk} \approx \left[\Delta T_{ijk} \cdot \Delta T_{ijk+1} \frac{\Delta T_{ijk} + \Delta T_{ijk+1}}{2}\right]^{\frac{1}{3}}. \tag{4.39}$$

While the approach temperatures are defined as

$$\Delta T_{ijk} = \max\{0, T_{ik} - T_{jk}\} \tag{4.40}$$

AS the max function is non-smooth and thus non differentiable at the points $T_{ik} = T_{jk}$, gPROMS® internally uses a smooth approximation. The exact for of which is unknown to the author.

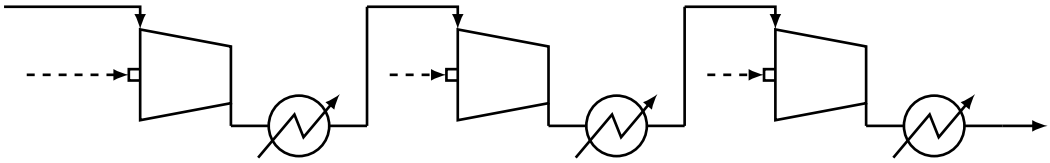

Figure 4.6: Multi-stage compression.

4.1.3 Compression & expansion

The issue of cooling the ambient air to process temperatures at around $90K$ is not an easy one. The main hindrance is, that a heat sink at this temperature level is not readily available. Lucky thermodynamics offer a different way to reach such temperatures. In order to do so, the ambient air first needs to be compressed and then expanded again. Cooling then occurs by either exploiting the *Joule-Thompson* effect or isentropic expansion. First a few comments are made about the compression stage, while afterwards the governing principles for cooling by expansion will be described.

Multi-stage compression

Compressors and expanders are among the most common process equipment. A multitude of processes utilizes them as primary or auxiliary units. In the context of cryogenic air separation the compression plays a major role, as it enables to reach temperatures needed for liquefying air and gases in general. As the compression of gases is always associated with a significant reduction in volume it requires large amounts of energy. Thus in addition to significantly contributing to the capital cost of the process the compression stage is responsible for the majority of the operating cost encountered in the ASU process.

The rigorous modeling of continuous flow machines in terms of unit operations poses great challenges. For specific units it may be undertaken by means of CFD simulations or employing characteristics diagrams, which require extensive experiments and can usually be obtained from the manufacturer. For the purposes of process design however a simpler approach with unit efficiencies is appropriate.

As a significant temperature increase goes along with the compression of air and in order to reduce the energy demand of the compression in general, it is beneficial, to use a multi stage compressor with inter-cooling as depicted in fig. 4.6. This yields a lower energy consumption as a single stage unit for the same compression ratio.

Subsequently the working equations for the compressor model used in the scope of this thesis are briefly summarized.

A trivial material and component balance around the compressor yields the outlet molar flow-rate F^{out} as well as the outlet overall composition z^{out}

$$0 = F^{in} - F^{out}, \tag{4.41}$$

$$0 = z_i^{in} - z_i^{out} \qquad i = 1 \dots n_C. \tag{4.42}$$

To calculate the mechanical work associated with the desired compression, first the isentropic case

$$S^{in} = S^{out} \tag{4.43}$$

is considered.

$$W_S = F^{in} \cdot (H^{in} - H^{out}) \tag{4.44}$$

$$W \cdot \eta^C = W_S \tag{4.45}$$

$$W_S = F^{in} \cdot H^{in}(T^{in}, p^{in}, z_i^{in}) - F^{out} \cdot H^{out}(T^{out}, p^{out}, z_i^{out}) \tag{4.46}$$

Pressure drop

$$p^{out} = p^{in} + \Delta p \tag{4.47}$$

Cooling by expansion

The liquefaction of gases requires temperatures well below ambient conditions. In order to reach such conditions one cannot utilize natural occurring coolants, but rather cooling effects that occur during the expansion of compressed gases. First we consider the expansion through an expansion valve or so called *Joule-Thompson* - valve. If we assume very good insulation of conditions this expansion can closely be approximated by an isenthalpic process ($h_1 = h_2$). To describe the change in temperature during isenthalpic expansion the *Joule-Thompson* coefficient

$$\mu_{JT} = \left(\frac{\partial T}{\partial p}\right)_h, \tag{4.48}$$

which denotes pressure derivative of the temperature at constant enthalpy can be considered. This can be transformed into

$$\mu_{JT} = \frac{1}{c_p}\left[T\left(\frac{\partial v}{\partial T}\right)_p - v\right] \tag{4.49}$$

If we employ the Peng-Robinson equation of state we can plot the isenthalpes for ambient air ($x_{N_2} = 0.7812$, $x_{O_2} = 0.2095$, $x_{Ar} = 0.0093$) in a PT-diagramm (fig. 4.7). One can easily see, that in certain ranges a pressure decrease will result in an increase in temperature, while for other regions in a decrease. It is interesting to mention that the non-idealities of a given gas give rise to this effect. For an ideal gas the temperature change at isenthalpic expansion would always be zero. Luckily for the cryogenic engineer real gases deviate from ideal behaviour especially at elevated pressures and low temperatures. It is therefore important to give some consideration to the thermodynamic model used to describe the properties of the system in question, as the non-ideal properties need to be captured appropriately.

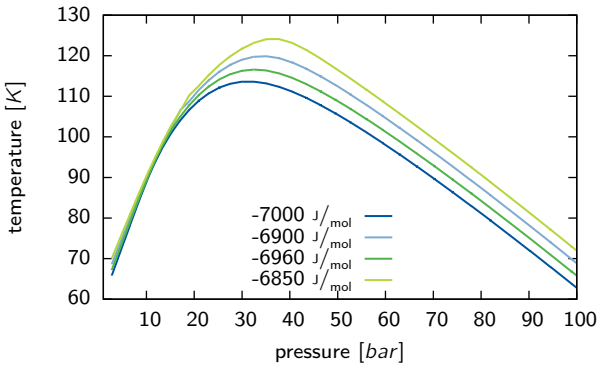

Figure 4.7: Isenthalpes computed by Peng-Robinson EOS.

A different way of expanding a compressed gas, is by letting it produce work in an fluid kinetic machine. If one assumes an adiabatic devices and disregards irreversible effects, this process can be viewed as isentropic. Analogous to the isenthalpic case an isentropic expansion coefficient can be defined

$$\mu_S = \left(\frac{\partial T}{\partial p}\right)_S = \frac{T}{c_p}\left(\frac{\partial v}{\partial T}\right)_p . \tag{4.50}$$

Here the derivative in the second form corresponds to the volumetric coefficient of thermal expansion β, which is always positive for gases, which in turn means, that an isentropic expansion will always result in an temperature decrease, whereas the isentropic expansion only led to a decrease in certain cases. Furthermore an isentropic expansion over the same pressure range will always result in lower temperatures than an isenthalpic expansion. Additionally work can be recovered. The reason that isentropic valves are most commonly used in liquefaction systems, is that those work producing machines cannot handle significant phase changes, which is after all the desired result of liquefaction.

Traditionally only the isenthalpic expansion had been used within the cryogenic air separation process, since – as mentioned before – the air needs to be liquefied in order to be fed into be distilled. However in modern process configurations the isentropic expansion is also considered, and partial streams are fed into the low pressure column in gaseous form.

4.2 Dynamic unit models

4.2.1 Distillation column model

The previously described column model is based on a steady state assumption. This means that all variables do not change with time. While a model like that offers valuable insight into the operation of a process many aspects remain unclear. In order to gain further insight into the process the dynamics have to be considered.

Due to that in this section a dynamic model of the ASU process will be developed.

First the balance equations have to be rewritten in dynamic form. To do so reservoir terms or holdups are introduced. Namely the component holdups n_{ij} and internal energy U_j for each stage.

$n_C - 1$ **component balances**

$$\frac{\mathrm{d}n_{ij}}{\mathrm{d}t} = \left(1 + s_j^V\right) \cdot V_j \cdot y_{i,j} + \left(1 + s_j^L\right) \cdot L_j \cdot x_{i,j} - V_{j+1} \cdot y_{i,j+1} - L_{j-1} \cdot x_{i,j-1} - \sum_{k=1}^{F^V} \zeta_{kj} \cdot F_j^V \cdot z_{i,j}^V - \sum_{l=1}^{F^L} \zeta_{lj} \cdot F_j^L \cdot z_{i,j}^L - \zeta_j^R \cdot V_N \cdot y_{iN}, \quad i = 1 \ldots n_C - 1, \quad j = 1 \ldots N, \quad k = 1 \ldots n_F, \quad l = 1 \ldots n_F. \tag{4.51}$$

Total internal energy balance

$$\frac{\mathrm{d}U_j}{\mathrm{d}t} = \left(1 + s_j^V\right) \cdot V_j \cdot h_j^V + \left(1 + s_j^L\right) \cdot L_j \cdot h_j^L - V_{j+1} \cdot h_{j+1}^V - L_{j-1} \cdot h_{j-1}^L - \sum_{k=1}^{F^V} \zeta_{kj} \cdot F_k^V \cdot h_j^{FV} - \sum_{l=1}^{F^L} \zeta_{lj} \cdot F_j^L \cdot h_j^{FL} - \zeta_j^R \cdot V_N \cdot h_N^V, \quad i = 1 \ldots n_C, \quad j = 1 \ldots n, \quad k = 1 \ldots n_F, \quad l = 1 \ldots n_F. \tag{4.52}$$

In addition to the balance equations further constituent equations need to be introduced. From the steady state model we know the equilibrium equations

$$y_{ij} = K_{ij} \cdot x_{ij}, \qquad i = 1 \ldots n_C \quad j = 1 \ldots n_S, \tag{4.53}$$

and the summation equations

$$1 = \sum_i^{n_c} y_{ij} \qquad j = 1 \ldots n_S, \tag{4.54}$$

$$1 = \sum_i^{n_c} x_{ij} \qquad j = 1 \ldots n_S. \tag{4.55}$$

Furthermore the accumulation of moles in each stage in vapour n_j^V and liquid n_j^L need to be considered with

$$n_{ij} = x_{ij} n_j^L + y_{ij} n_j^V \qquad i = 1 \ldots n_C \quad j = 1 \ldots n_S, \tag{4.56}$$

$$\tag{4.57}$$

These holdups are linked by the volume of a given stage V_{stage}. Thus the volume constraint can be written as

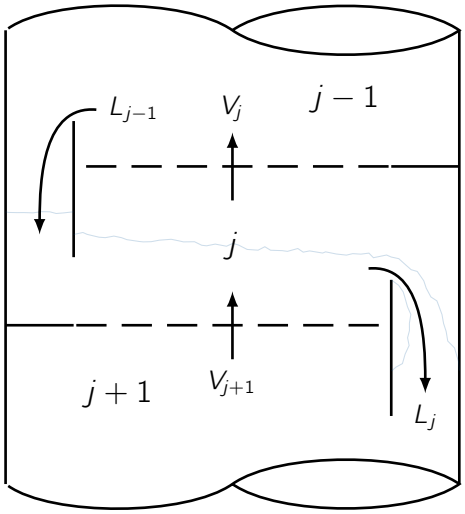

Figure 4.8: Column tray

$$V_{stage} = \frac{n_j^V}{\varrho_j^V} + \frac{n_j^L}{\varrho_j^L} \qquad j = 1 \dots n_S. \tag{4.58}$$

The internal energy in a stage corresponds to its enthalpy, reduced by pressure term

$$U_j = n_j^L \cdot h_j^L + n_j^V \cdot h_j^V - p_j \cdot V_{stage} \tag{4.59}$$

As we are no longer dealing in steady state hydraulic equations need to be introduces, which determine the liquid and vapour flow rates leaving a separation stage. As the mechanisms driving these flows might be very different depending on the type of internals used, it is not surprising that the corresponding equations are also very different. In the given model both trayed columns and columns with structured packing are employed.

Trayed hydraulics

Trayed column hydraulics can be approximated by the following system of equations. All equations presented here were taken from [1].

The liquid flow rates are calculated from the well established francis formula , derived from the law of Bernoulli and taking effects like bubbling into account

$$L_j = \frac{2}{3}\sqrt{2g}\varrho_j^L \ell_{weir} \Phi h_{ow}^{\frac{2}{3}} \qquad j = 1 \dots n_S. \tag{4.60}$$

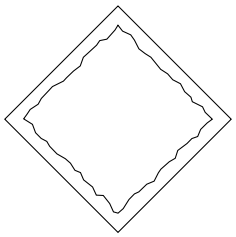

Where h_{ow} denotes the height of the liquid over the weir, which can be calculated from the froth height h_f and the weir height h_w

$$h_{ow} = h_f - h_w. \tag{4.61}$$

While the weir height is a tray design parameter the froth height is computed from the clear liquid height and the relative froth density

$$h_f = \frac{n^L \, MW^L}{A_{active} \, \varrho^L \, \Phi}. \tag{4.62}$$

Lastly in terms of liquid flow rates, the relative froth density is dependent on the degree of aeration within the liquid, expressed by the aeration factor β from an empirical equation

$$\beta_j = 1 - 0.3593 \left(\frac{V_{j-1} \, MW^V_{j-1}}{A_{active} \sqrt{\varrho_{j-1}}} \right)^{0.177709} \qquad j = 1 \ldots n_S, \tag{4.63}$$

$$\Phi_j = 2\beta_j - 1. \tag{4.64}$$

The pressure difference between stages is the driving force for the vapour streams. The pressure drop is modeled as having two contributions, the dray and wet pressure drop. While dry pressure drop stems from the vapour flowing through the holes with in tray, the wet pressure drop is caused by the liquid holdup on the stage.

$$p_j - p_{j+1} = h_j^{liq} \varrho_j^L g + 0.5 \xi \varrho_{j+1}^V \left(\frac{q_{j+1}^V}{A_h} \right)^2 \tag{4.65}$$

Structured packing hydraulics

Structured packings and their hydraulic behaviour are currently still under investigation. The number of available correlations for calculation of internal flow-rates is much more limited than for trays or even dumped packings. Among the most established models is the one developed by Bravo et al. [22] at the University of Texas. This model has been extended to be valid in the loading region and account for different types of packing material [14]. As main linking factor between vapour and

liquid flow-rates as well as the pressure drop, the liquid holdup has bee identified by the authors. It is expressed in dimensionless form h_t in terms of the corrugation side S, and the film thickness δ

$$h_L = \frac{4}{S}\delta. \tag{4.66}$$

One very important factor while estimating the hydraulic behaviour is the dry pressure drop per meter packing δp_{dry}. Within in the presented model it is estimated by

$$\delta p_{dry} = \left(\frac{\varrho^G}{\varrho_{air,1bar}}\right)^{0.4} \left(\frac{C_1 \varrho^G v_G^2}{S\epsilon^2(\sin\Theta)^2} + \frac{C_2 \mu_G v_G}{S^2 \epsilon \sin\Theta}\right) \tag{4.67}$$

Another perquisite for calculating the holdup is the knowledge of the amount of wetted area of the available surface area within the packing. It seems reasonable to assume that this will be dependent on the characteristic of the liquid flow through the packing. To characterize the current, well known dimensionless numbers are used. Namely *Weber* (We), *Froude* (Fr) and Reynolds (Re) numbers

$$We = \frac{v_L^2 \varrho_L S}{\sigma}, \tag{4.68}$$

$$Fr = \frac{v_L^2}{Sg}, \tag{4.69}$$

$$Re = \frac{v_L S \varrho_L}{\mu_L} \tag{4.70}$$

With that an approximation for the holdup correction factor F_t due to partial wetting can be expressed as

$$F_t = \frac{A_1 \left(We\, Fr\right)^{0.15} S^{A_2}}{Re^{0.2}\, \epsilon^{0.6} (1 - 0.93\cos\gamma)(\sin\Theta)^{0.3}} \tag{4.71}$$

$$h_L = \left(\frac{4F_t}{S}\right)^{\frac{2}{3}} \left\{ \frac{3\mu_L v_L}{\varrho_L \epsilon \sin\Theta g \left[\left(\frac{\varrho_L - \varrho_G}{\varrho_L}\right)\left(1 - \frac{\delta p}{\delta p_{flood}}\right)\right]} \right\}^{\frac{1}{3}} \tag{4.72}$$

4.3 Sizing & costing models

As discussed earlier economic consideration play a major role in process design. In order to account for the process economics the cost of the process to be implemented needs to be estimated at the design level. However as limited information is available estimation methods have to be employed. In sec. 3 the general approach for cost estimation of process equipment was introduced, where a specific value such as heat-exchange area or vessel size is used to approximate equipment cost. However for more specific units extended models are available, where statistical data is employed to yield a more realistic fit to cost data. The cost functions and correction factors presented in this chapter are, if not stated otherwise, taken from [23]. Also unless otherwise stated the unit cost is given for the year 2006 ($CE = 500$).

4.3.1 Destillation column

The cost of a given distillation column C_{column} is comprised of three main parts, the cost for the vessel or tower itself C_{tower}, the cost for platforms, ladders, manholes, and nozzles $C_{platform}$ and the cost for the internals $C_{internals}$

$$C_{column} = C_{tower} + C_{platform} + C_{internals}. \tag{4.73}$$

The determining factors for the cost of a tower are the construction material and the weight of the vessel. The material is considered by multiplying a base cost by a material factor f_M. Thus the cost for the tower can be approximated by

$$C_{tower} = f_M \cdot \exp\left[7.2756 + 0.18255 \cdot \ln(W_{tower}) + 0.02297 \cdot (\ln(W_{tower}))^2\right], \qquad 9000 \leq W_{tower} \leq 2 \tag{4.74}$$

In this correlation the weight W is measured in pounds ($[lbs]$)

For the support structures the following equation has bee presented

$$C_{platform} = 300.9 \cdot (d_{column})^{0.63316} \cdot (l_{column})^{0.80161}, \tag{4.75}$$

where both the diameter d_{column} and length l_{column} are measured in feet ($[ft]$).

The weight of the column is attained by calculation its volume and multiplying it by the mass density of the construction material $\tilde{\varrho}$

$$W_{column} = \pi(d_{column} + t_s)(l_{column} + 0.8 \cdot d_{column}) t_s \cdot \tilde{\varrho}. \tag{4.76}$$

It needs to be noted, that in this formula, all measurements have to be adjusted to the measurement of the density. Newly appearing is the shell thickness t_s of the tower. In order to compute this, several aspects can be considered.

The ASME pressure vessel code formula is used to compute the minimum thickness due to the design pressure p_D of a tower

$$t_p = \frac{p_D\, d_{column}}{2\,S\,E - 1.2 p_D}, \tag{4.77}$$

where S denotes the maximum allowable stress and E the fractional weld efficiency.

The design pressure is computed from the operating pressure p_O

$$p_D = \max\left\{10, \exp\left[0.60600 + 0.91615 \cdot \ln(p_O) + 0.0015655 \cdot (\ln(p_O))^2\right]\right\}, \tag{4.78}$$

It should be pointed out the the pressures in the previous equation are measured in pound per square inch gauge ($[psig]$).

In addition to the thickness due to pressure, it should be considered – especially for tall vessels – that the vessel might have to withstand external forces such as strong winds or earthquakes. To account for external effects a security addition t_w to the pressure thickness can be computed

$$t_w = \frac{0.22(d_{column} + 18) l_{column}^2}{S d_{column}}. \tag{4.79}$$

Therefor the total shell thickness amounts to

$$t_s = t_p + t_w. \tag{4.80}$$

In the previous equations the column diameter and length have frequently been used, however no mention has been made as to how to attain these values. While for a given design these values will be fixed, in the context of an optimization they need to be considered as decision variables. These decisions are closely linked to the choice of column internals. In case of the column height the procedure is very similar for columns with trays and structured packings. In case of the diameter however a clear distinction has to be made. This is due to the fact, that a decision regarding the diameter will have to ensure feasible column operations, which means it will have to be large enough to avoid flooding within the column. Consequently the procedures for determining height and diameter will be dealt with separately for each type of internals.

Trays

For a trayed column the height can be determined from the number of stages n_S used multiplied by the plate spacing h_{plate}. In addition however it needs to be ensured, that control of the columns is still possible. At the sump of the tower liquid will accumulate during operations. While in an ideal case the liquid level would be constant, that cannot be assumed. Regularly there are three different liquid levels defined in a column. The high level (HLL), normal level (NLL) and the low level (LLL). These levels are defined such that it sufficient time for the liquid to reach these levels (t_{min}^{HLL}, t_{min}^{NLL}, t_{min}^{LLL}) , if no liquid id withdrawn anymore, or no liquid comes down from the column. Furthermore the times for reaching the reboiler inlet and the lowest plat will ne necessary. What duration to reach those levels will be sufficient needs to be decided by a control engineer.

With these times and heights the height of the tower can be expressed as

$$l_{column} = n_S \cdot h_{plate} + \left(\sum_i t_{min}^i H^i \right) \cdot \frac{L_{n_S}}{A_{column} \varrho^L}. \tag{4.81}$$

This leaves the diameter to be determined. The most important factor to that regard is the vapour velocity within the tower. It is to be chosen such that no flooding or entrainment will occur. The following equation to compute these operation boundaries are taken from [17].

First the fractional entrainment factor ent_j for 80% flooding at each stage j needs to be calculated

$$ent_j = 2.24 \cdot 10^{-3} \cdot 2.377 \exp\left[-9.394 \cdot FLV_j^{0.314}\right], \qquad j = 1 \dots n_S. \tag{4.82}$$

Therein the Sherwood flow parameter FLV_j is used

$$FLV_j = \frac{\tilde{L}_j}{\tilde{V}_j} \cdot \sqrt{\frac{\tilde{\varrho}_j^V}{\tilde{\varrho}_j^L}}, \qquad j = 1 \dots n_S. \tag{4.83}$$

$$v_j^{flood} = 60 \cdot \left(\frac{\sigma_j^L}{20}\right) \cdot K1_j \cdot \sqrt{\frac{\tilde{\varrho}_j^L - \tilde{\varrho}_j^V}{\tilde{\varrho}_j^V}}, \qquad j = 1 \ldots n_S. \tag{4.84}$$

$$K1_j = 1.05 \cdot 10^{-2} + 0.1496 \cdot h_{plate}^{0.755} \cdot \exp\left[-1.463 \cdot FLV_j^{0.842}\right], \qquad j = 1 \ldots n_S. \tag{4.85}$$

With those values the minimum required column area for each stage A_j^{min} can be calculated

$$A_j^{min} = \frac{V_j}{\Psi_{flood} \varrho_j^V v_j^{flood}}, \qquad j = 1 \ldots n_S, \tag{4.86}$$

where Ψ_{flood} is a design parameter which determines the degree of flooding allowed and will usually have a value around 0.8.

Structured packings

The calculation of the column height is equivalent to the trayed case, with the one difference, that rather than using the plate spacing as the height for each stage a value called height equivalent to to theoretical plate ($HETP$) ist used. In terms of the column diameter the flooding velocity is determined by the flooding pressure drop as calculated in sec. 4.2.1.

4.3.2 Centrifugal pump

Pumps are among the most common units of process equipment. While there are several different kinds of pumps that can be used, the centrifugal pump is one of the most popular choices and denotes a very likely choice for the process conditions considered in this application. Hence other pump types will not be considered at this point.

Pump In terms of operations pumps are best described by the volumetric flow transported Q as well as the pump head H, the hight that needs to be overcome. Data taken from the company Mosanto was used to correlate the pump cost to a specific value

$$S = Q\sqrt{H}. \tag{4.87}$$

As a reference unit the base price C_B is estimated for a cast iron single-stage vertically split case at 3600 rpm

$$C_B = \exp\left\{9.7171 - 0.6019 \cdot \ln[S] + 0.0519(\ln[S])^2\right\}, \qquad 400 \leq S \leq 100000. \tag{4.88}$$

The most influential addition factors for the pump price are the material, which is accounted for in the material factor f_m, as well as the rotation, case split orientation (horizontal and vertical), the number of stages, covered flow rate range, pump head range and maximum motor power, which are all agglomerated in the type factor f_T. Values for these factors are given in tab. 4.3 and tab. 4.4.

number of stages	shaft rpm	case-split orientation	flow rate range ([gpm])	pump head range ([ft])	maximum power ([Hp])	type factor f_T
1	3600	VSC	50 - 900	50 - 400	75	1.00
1	1800	VSC	50 - 3500	50 - 200	200	1.50
1	3600	HSC	100 - 1500	100 - 450	150	1.70
1	1800	HSC	250 - 5000	50 - 500	250	2.00
2	3600	HSC	50 - 1100	300 - 1100	250	2.70
2+	3600	HSC	100 - 1500	650 - 3200	1450	8.90

Table 4.3: Pump type factors [23].

material of construction	material factor
cast iron	1.00
ductile iron	1.15
cast steel	1.35
bronze	1.90
stainless teel	2.00
Hastelloy C	2.95
monel	3.30
nickel	3.50
titanium	9.70

Table 4.4: Pump material factors [23].

Electric motor Separately from the pump itself the motor to drive the compression is considered. While the volumetric flow and the pump head certainly are valid choices to correlate motors for pumps especially, the power consumption is a more general specific value

$$P_C = \frac{P_T}{\eta_P \eta_M} = \frac{P_B}{\eta_M} \tag{4.89}$$

It can be calculated from the theoretic power of the pump P_T and the efficiencies η_P η_M. While an estimate for the expected power consumption might be already available at rather early design stages, the efficiencies will have to be correlated as well if resorting to average values is considered too coarse. Those correlations rely on the volumetric flow in gallons per minute ([gpm]) and the brake horse power $P_B = \frac{P_T}{\eta_P}$.

$$\eta_P = -0.316 + 0.24015 \cdot \ln[Q] - 0.01199 \cdot (\ln[Q])^2 \qquad 50 \leq Q \leq 5000 \tag{4.90}$$

$$\eta_M = 0.80 + 0.0319 \cdot \ln[P_B] - 0.00182 \cdot (\ln[P_B])^2 \qquad 1 \leq P_B \leq 1500 \tag{4.91}$$

After having calculated the power which the motor needs to supply its base cost of an open, drip-proof enclosed motor at 3600 rpm can be approximated by

$$\begin{aligned} C_B = \exp\big\{&5.8259 + 0.13141 \cdot \ln[P_C] + 0.053255 \cdot (\ln[P_C])^2 \\ &+ 0.028628 \cdot (\ln[P_C])^3 - 0.0035549 \cdot (\ln[P_C])^4\big\} \qquad 1 \leq P_C \leq 700 \end{aligned} \tag{4.92}$$

To adjust the cost for different types of electric motors the type factors from tab. 4.5

type motor enclosure	3600 rpm	1800 rpm
open, drip-proof enclosure, 1 to 700 Hp	1.0	0.9
totally enclosed, fan-cooled, 1 to 250 Hp	1.4	1.3
explosion-proof encosure, 1 to 250 Hp	1.8	1.7

Table 4.5: Type factors for different motor types.

Compressor

The cost of compressors is correlated with their respective power consumption measured in horsepower. Although not the most efficient type of compressor, centrifugal compressors are very popular in the process industry, as they are easily controlled an deliver a very steady flow. However as different types might be employed as well base cost correlations for centrifugal, reciprocation and screw compressors are given.

Centrifugal compressor

$$C_B = \exp\left\{7.5800 + 0.80 \cdot (\ln[P_C])\right\} \qquad 200 \leq P_C \leq 30000 \tag{4.93}$$

Reciprocating compressor

$$C_B = \exp\left\{7.9661 + 0.80 \cdot (\ln[P_C])\right\} \qquad 200 \leq P_C \leq 20000 \tag{4.94}$$

Screw compressor

$$C_B = \exp\left\{8.1238 + 0.7243 \cdot (\ln[P_C])\right\} \qquad 200 \leq P_C \leq 750 \tag{4.95}$$

Again as with most other equipment types correction factors are used to adjust for different realization of this piece of equipment. Here type of motor as well as the construction material have the biggest effects on the unit price and are explicitly considered.

$$C_p = f_D \, f_M \, C_B \tag{4.96}$$

The alternatives to the electric motor ($f_D = 1.0$) are a steam turbine ($f_D = 1.15$) or a gas turbine ($f_D = 1.25$). It should however be noted that aside from being the cheapest choice, the electric motor is also the most efficient. Thus the turbines are mostly considered, when process steam or combustion gas is easily available, such that the drawbacks might be eliminated by not having to supply the electric energy for the electric motor. In terms of construction material all base costs are for cast iron or carbon steel. Some appliances may require more resistant and also more expensive materials such as stainless steel ($f_M = 2.5$) or an nickel alloy ($f_M = 5.0$).

Reboiler / condenser

Reboiler and condenser can be characterized as heat exchangers, and be handled in the same way, as the main difference is weather heat is transferred to or from the process stream. In that sense they must be distinguished when considering the operating cost, as the cost for hot or cold auxiliary streams might differ significantly. As customary for heat exchangers the specific quantity for cost correlations is the necessary heat exchange area A measured in ft.

Again the construction material as well as the operating conditions have an effect on the final cost

$$C_p = f_P \, f_M \, C_B. \tag{4.97}$$

The correction for pressures f_P takes into account the operating pressure P_o and is computed by

$$f_P = 0.8510 + 0.1292 P_o + 0.0198 * P_o^2. \tag{4.98}$$

The material correction factor f_M

$$f_M = \tag{4.99}$$

Shell and tube heat exchanger

$$C_B = \exp\left\{11.667 - 0.8709 \cdot (\ln[A]) + 0.09005 \cdot (\ln[A])^2\right\} \tag{4.100}$$

Double pipe

$$C_B = \exp\left\{7.146 + 0.1600 \cdot (\ln[A])\right\} \tag{4.101}$$

4.4 Thermodynamic models

Aside from the unit operation models, the behaviour of materials in a process needs to be adequately accounted for. This is done by means of so called equations of state (EOS) and excess Gibbs energy models. In terms of thermodynamics there are only a limited amount of variables. Namely the pressure, density and temperature as well as composition. While equations of state can model a given system in the vapour as well as liquid phase, excess Gibbs energy models only account for the behaviour of a liquid and need to be used in conjunction with other models for the vapour phase. However they have shown considerable better performance for highly non-ideal systems [3]. As mentioned earlier (sec. **??**) it is essential to accurately capture the non-idealities of air in order to capture the liquefaction process. In the case of cryogenic air separation, the Peng-Robinson as well as the Benders equation of state have shown satisfactory performance. The Peng-Robinson equation

was chosen to be used in the presented model

$$p = \frac{RT}{V-b} - \frac{a_c\left[1+m\left(1-\sqrt{T_r}\right)\right]^2}{V^2+2bV-b^2} \tag{4.102}$$

$$m = 0.37464 + 1.54226\omega - 0.26992\omega^2 \tag{4.103}$$

$$a_c = 0.45724\frac{R^2T_c^2}{p_c} \tag{4.104}$$

$$b = 0.077796\frac{RT_c}{p_c} \tag{4.105}$$

$$\omega = -1 - \log_{10}\left(p_r^{sat}\right)_{T_r=0.7} \tag{4.106}$$

However the Peng-Robinson EOS relies on the so called one-fluid theory which models each fluid as pure. To model mixtures the pure component parameters have to be "mixed"

$$a = \sum_{i=1}^{C}\sum_{j=1}^{C} y_i y_j a_{ij}, \tag{4.107}$$

$$a_{ij} = \sqrt{a_i a_j}(1-k_{ij}), \tag{4.108}$$

$$b = \sum_{i=1}^{C} y_i b_i. \tag{4.109}$$

From that EOS numerous relevant properties such as excess enthalpy, fugacity coefficients or densities can be calculated. For a list of some relevant equations refer to sec. A.1.

4.5 Implementation

5 Conclusion and further research

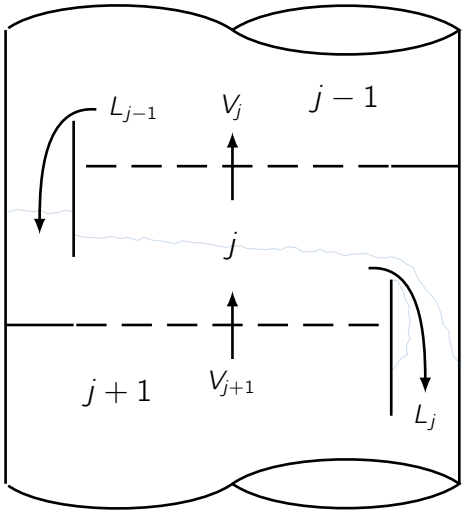
L_{j-1}
V_j
$j-1$
j
$j+1$
V_{j+1}
L_j

Bibliography

[1] *Distillation Tray Fundamentals*. Cambridge Univ Pr, 2009.

[2] Charles O. Akinlabi, Dimitrios I. Gerogiorgis, Michael C. Georgiadis, and Efstratios N. Pistikopoulos. Modelling, Design and Optimisation of a Hybrid PSA-Membrane Gas Separation Process. In V. Plesu and P. S. Agachi, editors, *17TH EUROPEAN SYMPOSIUM ON COMPUTER AIDED PROCESS ENGINEERING*, volume 24 of *Computer-Aided Chemical Engineering*, pages 363–370, SARA BURGERHARTSTRAAT 25 and PO BOX 211 and 1000 AE AMSTERDAM and NETHERLANDS, 2007. ELSEVIER SCIENCE BV.

[3] Andreas Pfennig. *Thermodynamik der Gemische*. Springer-Verlag, 2003.

[4] Mariana Barttfeld and Pío A. Aguirre. Optimal Synthesis of Multicomponent Zeotropic Distillation Processes. 1. Preprocessing Phase and Rigorous Optimization for a Single Unit. *Industrial & Engineering Chemistry Research*, 41(21):5298–5307, 2002.

[5] J. F. Boston. Inside-Out Algorithms for Multicomponent Separation Process Calculations: AkinlabiAkinlabi. In *Computer Applications to Chemical Engineering*, pages 135–151.

[6] J. F. Boston and S. L. Sullivan. A new class of solution methods for multicomponent, multistage separation processes. *The Canadian Journal of Chemical Engineering*, 52(1):52–63, 1974.

[7] W. F. Castle. Air separation and liquefaction: recent developments and prospects for the beginning of the new millennium. *International Journal of Refrigeration*, 25(1):158–172, 2002.

[8] J. J. J. Chen. Letter to the Editor: Comments on improvement on a replacement for the logarithmic mean. *Chemical Engineering Science*, 42:2488–2489, 1987.

[9] John M. Coulson and Raymond K. Sinnott. *Chemical engineering*. Pergamon Pr., Oxford and and Frankfurt, 3 edition, 1999.

[10] Guido Dünnebier and Constantinos C. Pantelides. Optimal Design of Thermally Coupled Distillation Columns. *Industrial & Engineering Chemistry Research*, 38(1):162–176, 1999.

[11] M. A. Duran and Ignacio E. Grossmann. Simultaneous optimization and heat integration of chemical processes. *AIChE Journal*, 32(1):123–138, 1986.

[12] Roger Fletcher and William Morton. Initialising distillation column models. *Computers & Chemical Engineering*, 23(11-12):1811–1824, 2000.

[13] Ignacio E. Grossmann, Pío A. Aguirre, and Mariana Barttfeld. Optimal synthesis of complex distillation columns using rigorous models. *Computers & Chemical Engineering*, 29(6):1203–1215, 2005.

[14] J. J. Gualito, F. J. Cerino, J. C. Cardenas, and J. A. Rocha. Design Method for Distillation Columns Filled with Metallic, Ceramic, or Plastic Structured Packings. *Industrial & Engineering Chemistry Research*, 36(5):1747–1757, 1997.

[15] Ernest J. Henley, J. D. Seader, and D. Keith Roper. *Separation process principles*. John Wiley & Sons, Chichester, 3 edition, op. 2011.

[16] Ravindra S. Kamath, Lorenz T. Biegler, and Ignacio E. Grossmann. Modeling multistream heat exchangers with and without phase changes for simultaneous optimization and heat integration. *AIChE Journal*, 58(1):190–204, 2012.

[17] A.I Lygeros and K.G Magoulas. Column Flooding and Entrainment. *Hydroc. Proc.*, 65(12):43–44, 1986.

[18] P. Mahapatra and B. W. Bequette. Process design and control studies of an elevated-pressure air separations unit for IGCC power plants: American Control Conference (ACC), 2010: American Control Conference (ACC), 2010 DOI -. *American Control Conference (ACC), 2010*, pages 2003–2008, 2010.

[19] Leonard M. Naphtali and Donald P. Sandholm. Multicomponent separation calculations by linearization. *AIChE Journal*, 17(1):148–153, 1971.

[20] Max Stone Peters, Klaus D. Timmerhaus, and Ronald E. West. *Plant design and economics for chemical engineers*. McGraw-Hill, New York, 5 edition, 2003.

[21] R. Prasad, F. Notaro, and D.R Thompson. Evolution of membranes in commercial air separation. *Journal of Membrane Science*, 94(1):225–248, 1994.

[22] J. Antonio Rocha, Jose L. Bravo, and James R. Fair. Distillation columns containing structured packings: a comprehensive model for their performance. 1. Hydraulic models. *Industrial & Engineering Chemistry Research*, 32(4):641–651, 1993.

[23] W. D. Seider, J. D. Seader, D. R. Lewin, and S. Widagdo. *Product and Process Design Principles: Synthesis, Analysis, and Evaluation*. J. Wiley, New York, 3 edition, 2010.

[24] Avinash R. Sirdeshpande, Marianthi G. Ierapetritou, Mark J. Andrecovich, and Joseph P. Naumovitz. Process synthesis optimization and flexibility evaluation of air separation cycles. *AIChE Journal*, 51(4):1190–1200, 2005.

[25] Phillip C. Wankat and Kyle P. Kostroski. Hybrid Membrane-Cryogenic Distillation Air Separation Process for Oxygen Production. *Separation Science and Technology*, 46(10):1539–1545, 2011.

[26] T.F Yee and Ignacio E. Grossmann. Simultaneous optimization models for heat integration—II. Heat exchanger network synthesis. *Computers & Chemical Engineering*, 14(10):1165–1184, 1990.

[27] Yu Zhu, Sean Legg, and Carl D. Laird. Optimal design of cryogenic air separation columns under uncertainty: Selected papers from the 7th International Conference on the Foundations of Computer-Aided Process Design (FOCAPD, 2009, Breckenridge, Colorado, USA. *Computers & Chemical Engineering*, 34(9):1377–1384, 2010.

A Appendix A

A.1 Peng-Robinson derived properties

The Peng-Robinson equation of state cab be rewritten as a cubic polynomial in terms of the compressibility factor $Z = \frac{pv}{RT}$

$$0 = Z^3 + \alpha Z^2 + \beta Z + \gamma \tag{A.1}$$
$$\alpha = B - 1 \tag{A.2}$$
$$\beta = A - 2B - 3B^3 \tag{A.3}$$
$$\gamma = B^3 + B^3 - AB \tag{A.4}$$
$$A = \frac{ap}{(RT)^2} \tag{A.5}$$
$$B = \frac{bp}{RT} \tag{A.6}$$

The *Joule-Thompson* factor cab be expressed as

$$\mu_{JT} = \frac{1}{c_p}\left[T\left(\frac{\partial v}{\partial T}\right)_p - v\right] \tag{A.7}$$

and in terms of the compressibility factor

$$\left(\frac{\partial v}{\partial T}\right)_p = \frac{R}{p}\left[T\left(\frac{\partial Z}{\partial T}\right)_p + Z\right] \tag{A.8}$$
$$\left(\frac{\partial Z}{\partial T}\right)_p = \frac{\left(\frac{\partial A}{\partial T}\right)_p (B - Z) + \left(\frac{\partial B}{\partial T}\right)_p (6BZ + 2Z - 3B^2 - 2B + A - Z^2)}{3Z^2 + 2(B-1)Z + (A - 2B - 3B^2)} \tag{A.9}$$
$$\left(\frac{\partial A}{\partial T}\right)_p = \frac{p}{(RT)^2}\left(a' - \frac{2a}{T}\right) \tag{A.10}$$
$$\left(\frac{\partial B}{\partial T}\right)_p = \frac{-bp}{RT^2} \tag{A.11}$$
$$a' = \frac{da}{dT} = \frac{1}{2}\sum_{i=1}^{C}\sum_{j=1}^{C} w_i w_j (1 - k_{ij})\left(\sqrt{\frac{a_j}{a_i}}a'_i + \sqrt{\frac{a_i}{a_j}}a'_j\right) \tag{A.12}$$
$$a'_i = \frac{da_i}{dT} = \frac{-m_i a_i}{\left[1 + m_i(1 - \sqrt{\frac{T}{T_{ci}}})\right]\sqrt{T T_{ci}}} \tag{A.13}$$

$$\ln \varphi = \frac{1}{RT} \int_0^p \left(V - \frac{RT}{p} \right) dp, \tag{A.14}$$

$$\ln \varphi = (Z-1) - \ln Z - \int_\infty^V \frac{Z-1}{V} dV \tag{A.15}$$

$$\ln \varphi_i = \frac{b_i}{b}(Z-1) - \ln \left[Z \cdot \left(1 - \frac{b}{V} \right) \right] + \frac{1}{bRT} \left[\frac{\sqrt{2} a b_i}{4b} - \sqrt{\frac{a a_i}{2}} \right] \ln \left(1 + \frac{b}{V} \right) \left(\frac{1 + \frac{b}{V}\left(1+\sqrt{2}\right)}{1 + \frac{b}{V}\left(1-\sqrt{2}\right)} \right) \tag{A.16}$$